Running title: Galactans retained by cellulose microfibrils

Corresponding author 1: Ewa J. Mellerowicz

E-mail: ewa.mellerowicz@slu.se

Address: Department of Forest Genetics and Plant Physiology, SLU, Umeå Plant Science Centre (UPSC), 90183, Umeå, Sweden

Tel: 46 90 786 8367

Fax: 46 90 786 8165

Corresponding author 2: Tatyana Gorshkova

E-mail: gorshkova@kibb.knc.ru

Address: Kazan Institute of Biochemistry and Biophysics, Kazan Scientific Centre, Russian Academy of Sciences, 420111, Kazan, Russia

Tel: +7 843 2925332

Fax: +7 843 2927347

Research area: Development and hormone action

Aspen tension wood fibers contain β-(1→4)-galactans and acidic arabinogalactans retained by cellulose microfibrils in gelatinous walls

Tatyana Gorshkova‡[1], Natalia Mokshina[1], Tatyana Chernova[1], Nadezhda Ibragimova[1], Vadim Salnikov[1], Polina Mikshina[1], Theodora Tryfona[3], Alicja Banasiak[2, 4], Peter Immerzeel[2], Paul Dupree[3], Ewa J Mellerowicz[2]‡

[1] Kazan Institute of Biochemistry and Biophysics, Kazan Scientific Centre, Russian Academy of Sciences, 420111, Kazan; E-mail: gorshkova@kibb.knc.ru; natalali@list.ru, tchernova@mail.knc.ru; nibra@yandex.ru; salnikov_russ@yahoo.com; p.mikshina@gmail.com

[2] Department of Forest Genetics and Plant Physiology, Swedish University of Agricultural Sciences, Umea Plant Science Centre, 90183 Umea, Sweden; E-mail: ewa.mellerowicz@slu.se; peter.immerzeel@slu.se

[3] Department of Biochemistry, University of Cambridge, Tennis Court Road, CB2 1QW, Cambridge, UK; E-mail: tt306@cam.ac.uk; pd101@bioc.cam.ac.uk

[4] Institute of Experimental Biology, University of Wroclaw, 50–328 Wroclaw, Poland; E-mail: balicja@biol.uni.wroc.pl

One-sentence summary:

Entrapment of pectic galactan and acidic arabinogalactan II within cellulose fibrils is a distinctive feature of aspen tension wood and other gelatinous fibers with contractile properties.

Footnotes:

Financial sources:
Swedish Governmental Agency for Innovation Systems (VINNOVA), the Swedish Research Council (VR), Russian Foundation for Basic Research (grant nos. 15-04-02560 and 15-04-05721), and the BBSRC (grant no. BB/G016240/1 and funds from the Sustainable Energy Centre Cell Wall Sugars Programme, BSBEC).

‡Corresponding authors: Ewa J. Mellerowicz, ewa.mellerowicz@slu.se, and Tatyana Gorshkova, gorshkova@kibb.knc.ru

Key words: *Populus*, hybrid aspen, secondary cell wall, tertiary cell wall, gelatinous fibers, tension wood, contractile walls

Abstract

Contractile cell walls are found in various plant organs and tissues such as tendrils, contractile roots and tension wood. The tension-generating mechanism is not known but is thought to involve special cell wall architecture. We previously postulated that tension could result from entrapment of certain matrix polymers within cellulose microfibrils. As reported here, this hypothesis was corroborated by sequential extraction and analysis of cell wall polymers that are retained by cellulose microfibrils in tension wood and normal wood of hybrid aspen (*Populus tremula* L. x *tremuloides* Michx.). β-(1→4)-Galactan and type II arabinogalactan were the main large matrix polymers retained by cellulose microfibrils that were specifically found in tension wood. Xyloglucan was detected mostly in oligomeric form in the alkali-labile fraction and was enriched in tension wood. β-(1→4)-Galactan and rhamnogalacturonan I backbone epitopes were localized in the gelatinous cell wall layer. Type II arabinogalactans retained by cellulose microfibrils had a higher content of (Me)GlcA and Gal in tension wood than in normal wood. Thus, β-(1→4)-galactan and a specialized form of type II arabinogalactan are trapped by cellulose microfibrils specifically in tension wood, and are thus the main candidate polymers for the generation of tensional stresses by the entrapment mechanism. We also found high β-galactosidase activity accompanying tension wood differentiation, and propose a testable hypothesis that such activity might regulate galactan entrapment and thus mechanical properties of cell walls in tension wood.

Introduction

Contractile cell walls found in plant organs and tissues such as tendrils, contractile roots and tension wood (TW) have remarkable functions and properties. Their traits have been most intensely studied in TW of hardwoods, where they provide negative gravitropic response capacities to stems with secondary growth, as recently reviewed by Mellerowicz and Gorshkova (2012). These properties are conferred by TW fibers, which in many species contain a so-called gelatinous (G) cell wall layer (Norberg and Meier, 1966; Clair et al., 2008). G-layers are formed following the deposition of xylan type secondary cell wall layer(s) and thus can be considered tertiary layers (Wardrop and Dadswell, 1948). They are almost or completely devoid of xylan and lignin, and have very high cellulose contents (up to 85%). However, several other polymers appear to be present in TW G-layers, according to recent chemical analyses of isolated G-layers (Nishikubo et al., 2007; Kaku et al., 2009) and immunohistochemical labeling of TW sections (Bowling and Vaughn, 2008; Arend, 2008). Notably, xyloglucan (XG) has been found in G-layers of poplar TW (Nishikubo et al., 2007), and at the boundary between S and G-layers (Baba et al., 2009; Sandquist et al., 2010). It is also important for tension creation (Baba et al., 2009). However, it is not detectable in mature G-layers by monoclonal antibodies or XG-binding modules (Nishikubo et al., 2007; Baba et al., 2009; Sandquist et al., 2010).'

Structurally similar G-layers have been also identified in phloem fibers in many fibrous crops, such as flax, hemp, and ramie (Gorshkova et al., 2012). These fibers occur in bundles that can be isolated for biochemical analysis. G-layers in fibers from diverse sources have a very similar structure, being largely composed of cellulose (with axial microfibril orientation, high degrees of crystallinity and large crystallite sizes), lacking xylan and lignin (Mellerowicz et al., 2001; Pilate et al., 2004; Gorshkova et al., 2010, 2012), and having high water contents (Schreiber et al., 2010). In phloem fibers, the G-layers become very prominent, reaching thicknesses up to 15 μm and occupying over 90% of cell walls' total cross-sectional areas (Cronier et al., 2005). Pectic β-(1→4)-galactan with complex structures has been shown to be the major matrix polysaccharide of isolated phloem fibers in flax (Gorshkova et al., 2004; Gorshkova and Morvan, 2006; Gurjanov et al., 2007). Some of it is so strongly retained within cellulose that it cannot be extracted by concentrated alkali and can only be obtained after cellulose dissolution (Gurjanov et al., 2008). Such galactan is therefore a prime candidate for a polymer entrapped by cellulose microfibrils during crystallization that could substantially contribute to contractile properties of cellulose in G-layers according to recently formulated models (Mellerowicz et al., 2008; Mellerowicz and Gorshkova 2012). Furthermore, Roach et al. (2011) have shown that trimming of β-(1→4)-galactan by β-galactosidase is important for final

cellulose crystallization, formation of G-layer structure and (hence) stems' mechanical properties.

There is also immunocytochemical evidence for the presence of β-(1→4)-galactan and type II arabinogalactan (AG-II) in G-layers of TW fibers (Arend, 2008; Bowling and Vaughn, 2008). In addition, high molecular weight branched galactans have been isolated from TW of *Fagus sylvestris* (Meier, 1962) and *F. grandifolia* (Kuo and Timmel, 1969), with estimated degrees of polymerization (DP) of ca. 300 and complex structure, probably including both β-(1→4)- and β-(1→6)-types of linkages, although their exact nature remains unknown. Furthermore, galactose (Gal) has been identified as one of the major sugars after glucose (Glc) and xylose (Xyl) in hydrolyzates of isolated *Populus* G-layers (Furuya et al., 1970; Nishikubo et al., 2007) and the Gal content of cell walls is a proposed indicator of the extent of TW development in beech (Ruel and Barnoud, 1978). However, subsequent linkage analyses identified only 2-, and 3,6-linked Gal in poplar TW G-layers (Nishikubo et al., 2007), while in flax fibers 4-linked Gal is the main component (Gorshkova et al., 1996, 2004; Gurjanov et al., 2007, 2008). Thus, the type(s) of galactans present in poplar TW remains unclear, and the galactans have not been previously shown either to have a rhamnogalacturonan-I (RG-I) backbone or to be strongly retained by cellulose microfibrils, as demonstrated for flax gelatinous fibers.

To improve understanding of cell wall properties in TW and their contraction mechanism, in the study presented here we tested aspects of the recently proposed entrapment model (Mellerowicz et al., 2008; Mellerowicz and Gorshkova, 2012). According to this model, contraction is driven by the formation of larger cellulose structures, sometimes called macrofibrils, via interactions of cellulose microfibrils in the G-layer with each other and forming inclusions containing matrix polymers. This would induce tension within cellulose through the stretching of microfibrils required to surround the inclusions. The model is compatible with available data on the structure and action of gelatinous walls, but the main assumption, that polymers are trapped inside crystalline cellulose, such as that found in flax, has not been previously tested. Therefore, we compared matrix polymers retained by cellulose microfibrils in normal wood (NW) and TW of the model hardwood species *Populus* that forms TW with G-fibers. For this purpose we used a combination of sequential cell wall extractions, similar to those previously used to characterize flax G-fibers (Gurjanov et al, 2008), followed by fractionation of polymers by size exclusion chromatography (SEC), immunological analyses and oligosaccharide profiling by Polysaccharide Analysis using Carbohydrate gel Electrophoresis (PACE). The results reveal the main polymers of cellulose-retained fractions and key differences between NW and TW. Comparison of our results and previous findings also

indicates that there are both similarities and differences in the constitution of G-fibers in aspen and flax. An updated model of the contractile G-layer of TW fibers based on the data is presented.

Results

Sequential cell wall extraction and analysis reveals basic differences between normal and tension wood

To induce TW, aspen trees were tilted at approx. 45 degrees from vertical for several weeks. This induced formation of G-fibers with very prominent G-layers, while fibers in NW of upright control trees predominantly had solely secondary walls (S-fibers) (Fig. 1A). After milling, to the same particle size, TW and NW samples had distinct textures (Fig. 1B). Monosaccharide analysis of total trifluoroacetic acid (TFA)-hydrolysable sugars in cell walls of these samples revealed that TW had considerably lower proportions of Xyl (although it remained the major sugar) and Man than NW (Fig. 1C). In contrast, the proportion of Glc (the second most abundant monomer in the hydrolysates), which could at least partly originate from amorphous cellulose and XG, was higher in TW (203±30 mg/g dry weight, DW) than in NW (110±32 mg/g DW). Proportions of Gal, Rha, and GalA were also higher in TW than in NW.

To characterize cell wall polysaccharides more specifically, NW and TW samples were fractionated by the sequential extraction procedure shown in Fig. S1 into: buffer-soluble polymers, ammonium oxalate-extractable polymers, 4 M KOH-extractable polymers, cellulose-retained polymers, lignin-bound polymers, and lignin. Yields of the fractions obtained from NW and TW considerably differed (Table 1), but cellulose, KOH-extractable polymers, and lignin were the most abundant fractions in both cases. As expected, KOH-extractable polymers and lignin contents were lower, while cellulose contents were higher, in TW than in NW. Buffer-extractable polymers were also considerably more abundant (but still a minor fraction) in TW. The cellulose-retained non-glucose polymers constituted approx. 2% of cell wall dry weight in both wood types.

To gain an oversight of the composition of polysaccharides in the fractions, their monosaccharide compositions were first determined (Table 2). The major constituents of the buffer-soluble fraction, according to monosaccharide analysis, were Gal, Rha and GalA, suggesting the presence of pectic galactan. In both wood types the 4 M KOH fraction contained mostly Xyl, which was initially measured together with Man (Xyl(Man)). However, its content was lower in TW (Table 2). Separation of Xyl and Man in further subsequent analysis of the fraction indicated that Man constituted around 12% of Xyl(Man), in both NW and TW. TFA-hydrolysis of the non-KOH-extractable cell wall material yielded mainly Glc. Non-glucose monosaccharides of this fraction amounted to 19±3 and 22±6 mg/g DW in NW and TW, respectively, Xyl(Man) accounting for ca. half of these amounts. Gal was the next most abundant sugar in TW samples, in which its proportion was twice as high as in NW (Table 2). Cellulose-retained matrix polysaccharides (excluding Glc) contributed around a third of the total

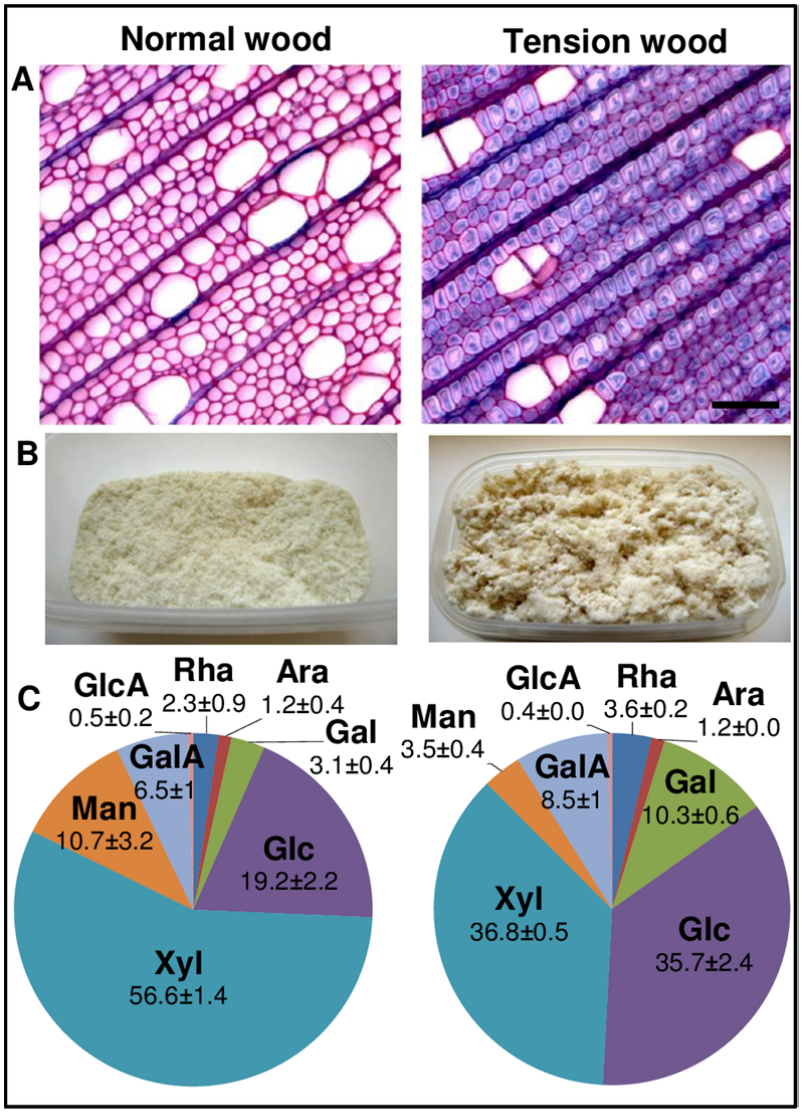

Figure 1. Anatomy (A), macroscopic appearance (B) and monosaccharide composition (C) of normal and tension wood. **A,** Light microscopy images of normal wood from an upright tree and tension wood from a tilted tree stained with alcian blue-safranin. Note the prominent non-lignified G-layers stained blue in tension wood, and lignified compound middle lamella and S layers stained red in both normal and tension wood. Bar = 50 mm. **B,** Appearance of normal and tension wood after milling. **C,** Monosaccharide composition (mol %) of TFA hydrolyzates of normal and tension wood.

yield of monosaccharides from the KOH-unextractable fraction and amounted to 7±2 and 8±4 mg/g DW in NW and TW samples, respectively. Gal was twice as abundant in polymers of this fraction from TW as in corresponding polymers from NW, in both absolute amounts and proportions (35±3 versus 17±2 mol %; Table 2). Some carbohydrates (5±2 and 3±1 mg/g DW in

NW and TW, respectively) remained in the pellet after all the applied extraction procedures, and were presumably linked to lignin. The yield of this fraction was lower from TW samples, mainly due to reductions in Glc amounts, while proportions of other sugars in the TW and NW fractions were similar (Table 2).

The fractions were subsequently subjected to immunodot analysis using antibodies recognizing cell wall matrix polysaccharides likely to be present according to their monosaccharide compositions. These were: LM11 for β-(1→4)-xylan (McCartney et al., 2005), LM15 for XG (Marcus et al., 2008), JIM14 for arabinogalactan protein (AGP) (Knox et al., 1991), LM5 for β-(1→4)-galactan (Jones et al., 1997) and RU2 for RG-I backbone (Ralet et al., 2010). Sugar contents of samples of total fractions were equalized, and the samples were used in several dilutions. Images of the membrane with immunodots obtained for buffer-soluble, KOH-extractable and cellulose-retained polysaccharides are presented in Fig. 2. Most β-(1→4)-xylan, as indicated by LM11 antibody binding, was extracted by 4 M KOH, some appeared in the cellulose-retained fraction, but none was detected in the buffer-soluble fraction. Xylan signals were weaker in the KOH-extractable fraction of TW than in the corresponding NW fraction, but similar in the cellulose-retained fraction of both wood types. JIM14 labeling, indicative of arabinogalactan, appeared in all analyzed fractions, but more strongly in NW than in TW samples. LM15 labeling indicated the presence of trace amounts of XG in the KOH-extractable fraction of NW, and greater amounts in this fraction of TW. There was also a trace of XG in the cellulose-retained fraction of TW, but not NW. Immunodot analysis with LM5 revealed higher amounts of β-(1→4)-galactan in TW than in NW samples, in all analyzed fractions (but particularly the cellulose-retained fraction), and this was the most significant difference between them. Immunolabeling with RU2 antibody confirmed the presence of rhamnogalacturonan I backbone in all analyzed fractions, and RU2 signal was substantially stronger in the cellulose-retained fraction of TW than in the corresponding NW fraction.

These results indicate three major differences between NW and TW. TW contains more buffer-soluble polymers and cellulose, but less hemicelluloses and lignins (Table 1; Fig. 1). There are differences in monomeric composition between NW and TW in all of the fractions (corroborated by the observed differences in immunolabeling with specific antibodies). TW samples (of all fractions) appear to contain significantly higher levels of β-(1→4)-galactan.

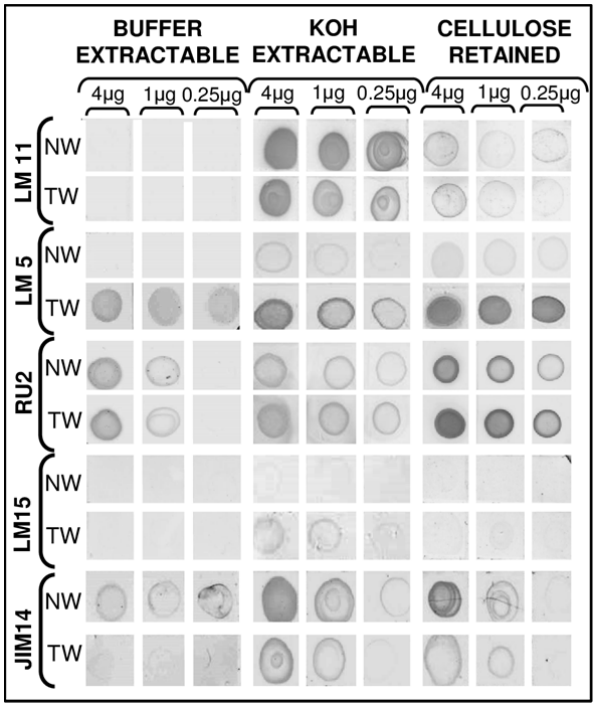

Figure 2. Immunodot analysis of cell wall polysaccharides in buffer-extractable, KOH-extractable and cellulose-retained (obtained after cellulase treatment) fractions of normal and tension wood (NW and TW, respectively) with antibodies recognizing: (1→4)-β-xylan (LM11) (McCartney et al., 2005), (1→4)-β-galactan (LM5) (Jones et al.1997), rhamnogalacturonan I backbone (RU2) (Ralet et al., 2010), the XXXG motif of xyloglucan (LM15) (Marcus et al., 2008), and an unknown epitope of arabinogalactan protein (JIM14) (Knox et al., 1991). Total fractions (aliquots taken before gel-filtration) were used for analysis. 4 µg, 1 µg and 0.25 µg on top of the membrane images indicate the amount of carbohydrates spotted on each vertical line of dots.

Size exclusion chromatography fractionation of different extracts and characterization of subfractions reveal differences in galactans between normal and tension wood

To compare mass-distributions of polymers in NW and TW samples, the polysaccharide fractions were subjected to gel-filtration, divided into high and low molecular weight subfractions according to the major peaks, then analyzed in more detail.

Buffer-soluble polymers

The buffer-soluble fraction had substantial polymer contents in TW but very low contents in NW samples. The polymers purified by precipitation eluted in the 10-200 kDa region (Fig. 3A), with a considerable proportion of carbohydrates present in the oligomeric region (<5 kDa). Gal was the major monomer of the polymeric fraction, and its proportion was higher in TW than in NW (Fig. 3B). The oligomeric TW subfraction contained mostly Gal, GalA, and Rha, suggesting enrichment in RGI oligosaccharides. Results of the sugar composition (Table 2) and immunodot analyses (Fig. 2) indicate that the main polymer of the buffer-soluble fraction in TW is high molecular weight β-(1→4)-galactan. Some AG-II and oligomeric RGI were also detected.

To investigate the nature of those galactans further, we structurally characterized them by PACE. For the analysis of AG-II, high molecular weight subfractions of TW and NW (Fig. 3A) were adjusted to contain equal amounts of Ara, then hydrolyzed with two AG-II specific enzymes. One was exo-β-1,3-galactanase, which hydrolyses terminal β-(1→3)-Gal linkages, but can bypass branching points liberating any β-(1→6)-galactan side chains with various DPs

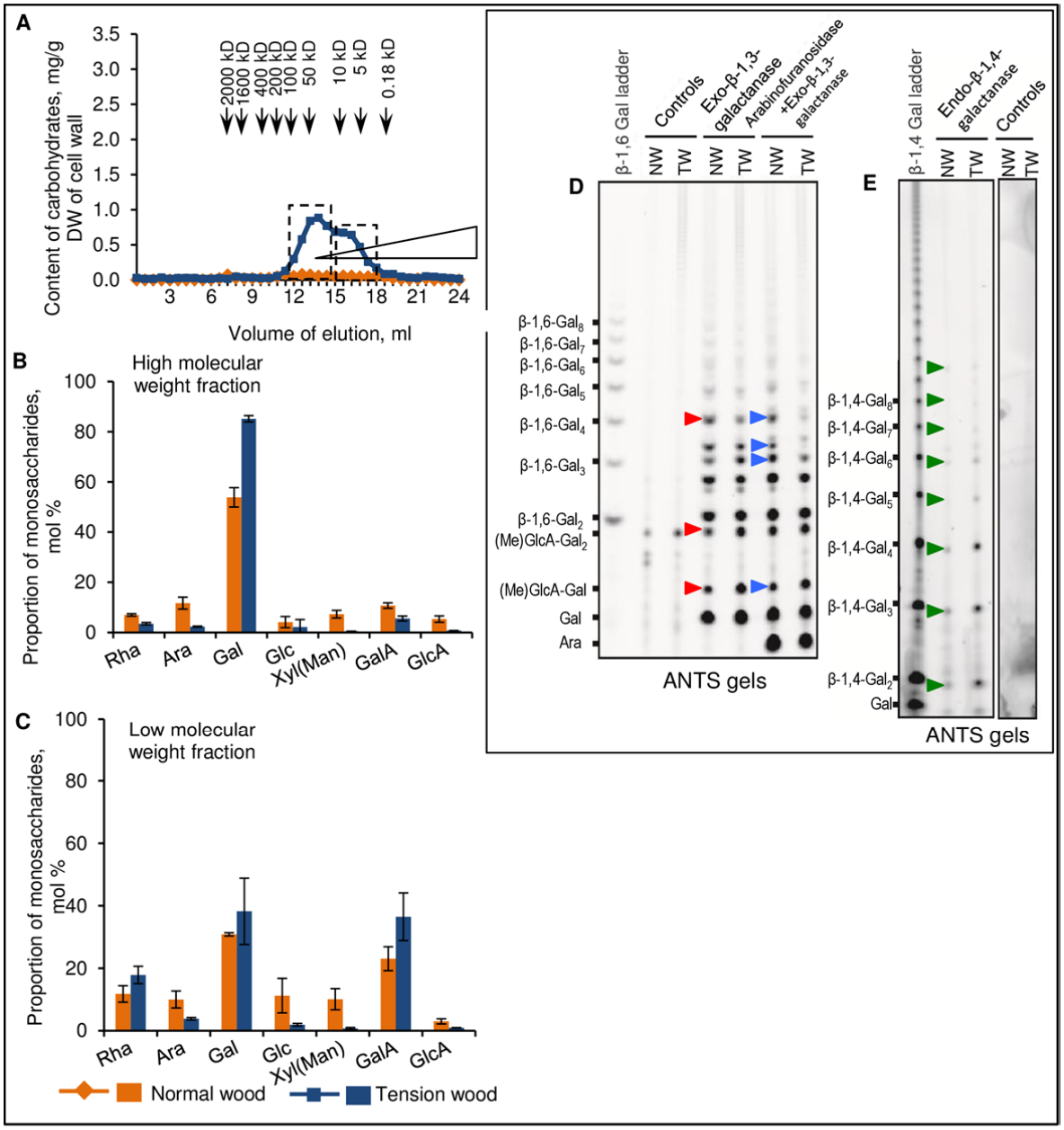

Figure 3. Analysis of two subfractions of buffer-extractable polysaccharides of normal and tension wood (NW and TW, respectively). **A,** Elution profile with designation of two subfractions. **B and C,** Proportions of monosaccharides obtained after TFA hydrolysis of high and low molecular weight fractions, respectively. **D and E,** Oligosaccharide fragments obtained after enzymatic digestion and separation by PACE on ANTS gels. For the type II arabinogalactan analysis, the high molecular mass subfractions of NW and TW were adjusted to equalize their total Ara contents and digested with exo-β-(1→3)-galactanase alone or in combination with arabinofuranosidase (D). For β-(1→4)-galactan analysis, the same samples were adjusted to equalize total sugar amounts and digested with endo-β-(1→4)-galactanase (E). Controls are the samples without enzymatic digestion to check for background signals. Bands with differing yields from NW and TW samples are marked by arrowheads: (red) - released with exo-β-(1→3)-galactanase, (blue) - by α-arabinanase followed by exo-β-(1→3)-galactanase, and (green) – by endo-β-(1→4)-galactanase. Error bars in graphs B and C show the standard error of the mean, n=3 biological repeats.

(Tsumuraya et al., 1990). The other was α-arabinofuranosidase, which removes terminal Ara residues (Takata et al., 2010). The resulting oligosaccharides were analyzed by gel electrophoresis. As shown in Fig. 3D, the high molecular weight subfractions of both NW and TW samples were susceptible to the enzymatic treatment, which released a ladder of

oligosaccharides with DP ranging from 1 to 8. Some of the oligosaccharides co-migrated with known standards (Tryfona et al., 2010, 2012) while others were of unknown identity. However, there were substantial differences in abundance of the oligosaccharides released from the NW and TW samples. In particular, higher amounts of (Me)GlcA-Gal and (Me)GlcA-Gal_2, and lower amounts of β-(1→6)-Gal_4 were released by exo-β-(1→3)-galactanase from TW samples (Fig. 3D, red arrowheads). In addition, lower amounts of β-(1→6)-Gal_4, β-(1→6)-Gal_3 and an unidentified product, but higher amounts of (Me)GlcA-Gal (Fig. 3D, blue arrowheads) were released by a combination of α-arabinanase followed by exo-β-(1→3)-galactanase from TW samples. These results indicate that there are structural differences in buffer-soluble AG-II between NW and TW.

To investigate the nature of β-(1→4)-galactans in the high molecular weight subfraction, NW and TW samples with equal total sugar contents were hydrolyzed with endo-β-(1→4)-galactanase and the resulting oligosaccharides were analyzed by gel electrophoresis (Fig. 3E). The endo-β-(1→4)-galactanase hydrolysis resulted in a number of oligosaccharides with apparent DP ranging from 1 to 8, which comigrated with known standards. TW samples yielded considerably more of these fragments than NW samples (Fig. 3E, green arrowheads). Thus, β-(1→4)-galactan is far more abundant in TW (as TW samples have much higher buffer-extractable contents) than in NW. The galactanase used cuts unbranched β-(1→4)-galactan into products with DP 1-3 (Barton et al., 2006), and corresponding bands were the most intense. However, higher DP products were also detected, suggesting the presence of branching points or other obstacles for the enzyme's action. TW samples yielded more abundant and diverse products of this type, suggesting that β-(1→4)-galactan has a more complex structure in TW than in NW.

KOH-extractable polysaccharides

Some of the polymers in the major, KOH-extractable, fractions of both TW and NW samples eluted in the > 500 kDa region and constituted the highest-molecular mass subfraction of all analyzed polysaccharides (Fig. 3, Fig. 4, Fig. 5). The rest eluted between 5 and 100 kDa (Fig. 4A).

The sugar composition of the high molecular weight subfraction was similar in TW and NW samples (Fig. 4B). In both cases, Xyl(Man) were the most abundant sugars. Accordingly, the LM11 antibody specific for β-(1→4)-xylan bound strongly to subfractions isolated from both NW and TW samples (Fig. 4D). To investigate whether mannans were present in the samples, the LM21 antibody that specifically binds β-(1→4)-mannan (Marcus et al., 2010) was used. Immunodot analysis confirmed the presence of β-(1→4)-mannan epitopes in this subfraction

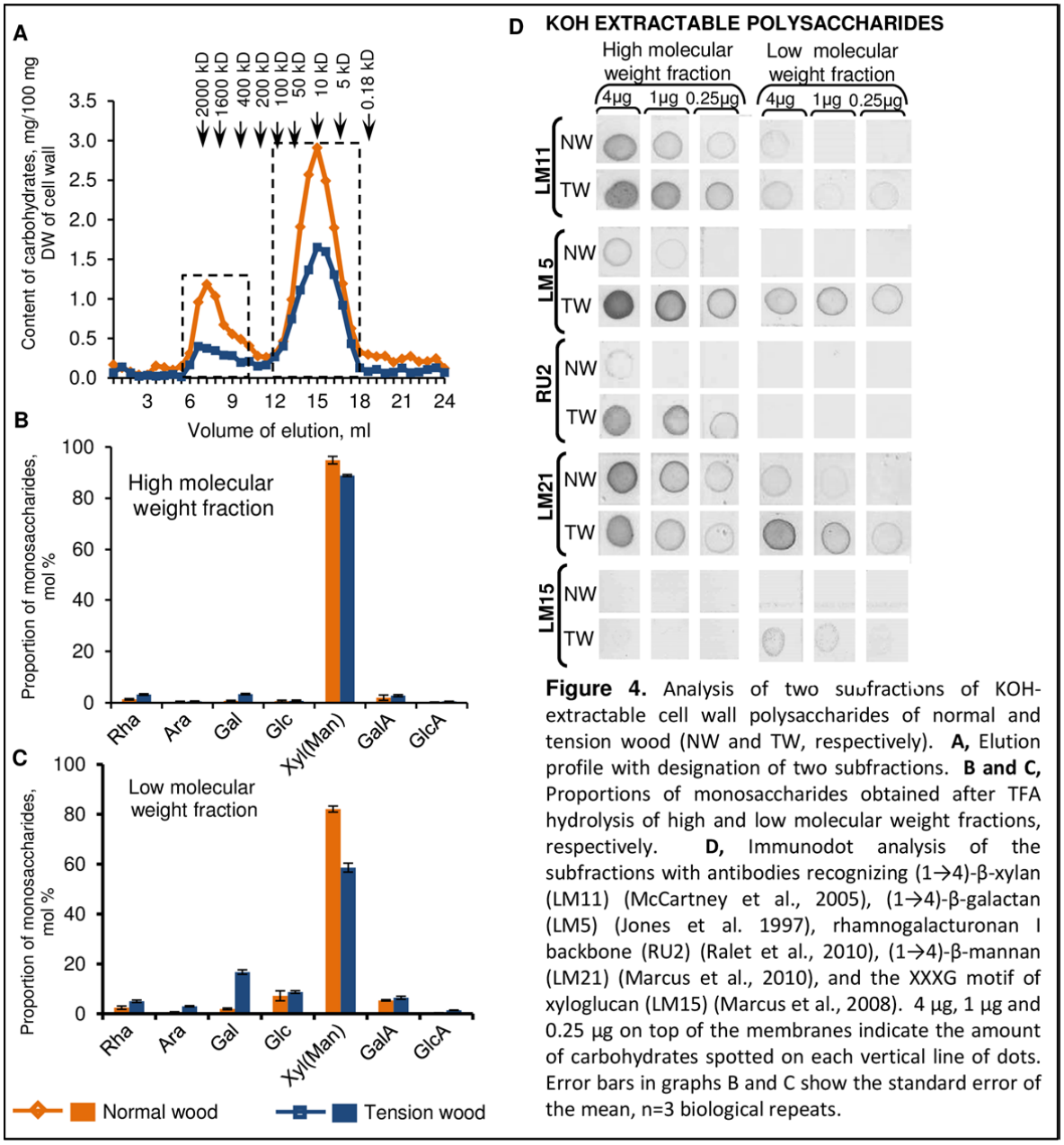

Figure 4. Analysis of two subfractions of KOH-extractable cell wall polysaccharides of normal and tension wood (NW and TW, respectively). **A,** Elution profile with designation of two subfractions. **B and C,** Proportions of monosaccharides obtained after TFA hydrolysis of high and low molecular weight fractions, respectively. **D,** Immunodot analysis of the subfractions with antibodies recognizing (1→4)-β-xylan (LM11) (McCartney et al., 2005), (1→4)-β-galactan (LM5) (Jones et al. 1997), rhamnogalacturonan I backbone (RU2) (Ralet et al., 2010), (1→4)-β-mannan (LM21) (Marcus et al., 2010), and the XXXG motif of xyloglucan (LM15) (Marcus et al., 2008). 4 µg, 1 µg and 0.25 µg on top of the membranes indicate the amount of carbohydrates spotted on each vertical line of dots. Error bars in graphs B and C show the standard error of the mean, n=3 biological repeats.

(Fig. 4D). In addition, it contained low amounts of Rha and Gal (more clearly detected in TW samples than in NW samples). The immunoblot analysis also revealed the presence of β-(1→4)-galactan and rhamnogalacturonan I backbone, which is consistent with the presence of RG-I polymer in this subfraction. Signals from LM5 and RU2 antibodies were far stronger in TW than in NW samples, indicating that RG-I, and β-(1→4)-galactan epitopes, are more abundant in TW (Fig. 4D).

Xyl(Man) were also the most abundant sugars in the low molecular weight subfraction, but Rha, Ara, Gal, Glc and GalA were also detected (Fig. 4C). More Gal and less Xyl(Man) was found in TW than in NW. Immunoblot signals revealed the presence of β-(1→4)-xylan, β-(1→4)-mannan, β-(1→4)-galactan and XG in this subfraction, of which β-(1→4)-galactan and XG

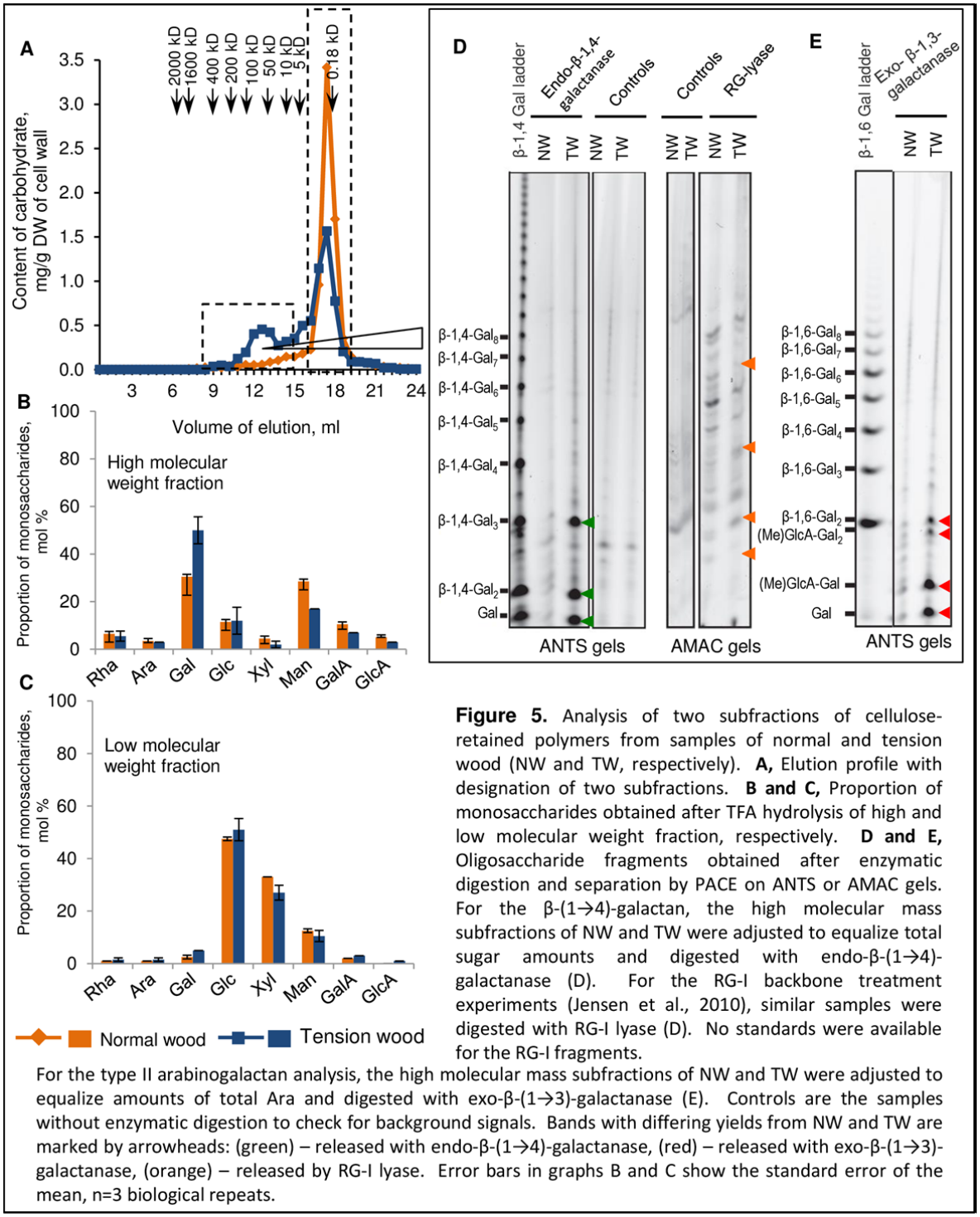

Figure 5. Analysis of two subfractions of cellulose-retained polymers from samples of normal and tension wood (NW and TW, respectively). **A,** Elution profile with designation of two subfractions. **B and C,** Proportion of monosaccharides obtained after TFA hydrolysis of high and low molecular weight fraction, respectively. **D and E,** Oligosaccharide fragments obtained after enzymatic digestion and separation by PACE on ANTS or AMAC gels. For the β-(1→4)-galactan, the high molecular mass subfractions of NW and TW were adjusted to equalize total sugar amounts and digested with endo-β-(1→4)-galactanase (D). For the RG-I backbone treatment experiments (Jensen et al., 2010), similar samples were digested with RG-I lyase (D). No standards were available for the RG-I fragments.

For the type II arabinogalactan analysis, the high molecular mass subfractions of NW and TW were adjusted to equalize amounts of total Ara and digested with exo-β-(1→3)-galactanase (E). Controls are the samples without enzymatic digestion to check for background signals. Bands with differing yields from NW and TW are marked by arrowheads: (green) – released with endo-β-(1→4)-galactanase, (red) – released with exo-β-(1→3)-galactanase, (orange) – released by RG-I lyase. Error bars in graphs B and C show the standard error of the mean, n=3 biological repeats.

were only detected in TW, while β-(1→4)-xylan and β-(1→4)-mannan were detected in both TW and NW (Fig. 4).

The separation of polymers into two clear peaks (Fig. 4A), each of which contained Xyl(Man) and was labeled in immunodot analysis by LM11 and LM21 antibodies, suggested the presence of two populations of β-(1→4)-xylan and β-(1→4)-mannan molecules in the KOH-extractable fraction of both NW and TW. These populations might differ in the presence of some intermolecular interactions or linkages. Similarly, there were two populations of β-(1→4)-

galactan, both of which were far more abundant in TW. XG was only detected in TW as an oligomer or low molecular weight polysaccharide.

Cellulose-retained polymers

Polymers isolated from the alkali-unextractable pellets by dissolution with LiCl in DMA and subsequent cellulase treatment were separated by gel-filtration into two major subfractions with very distinct compositions (Fig. 5A). One was represented by a peak in the 50-200 kDa molecular mass region and more pronounced in TW samples, while the other eluted mainly in the < 5 kDa region and was less pronounced in TW samples than in NW samples. The latter had very similar monomeric sugar constitutions in NW and TW samples, with high Glc and Xyl contents, suggesting the presence of oligomeric fragments of xylan and probably contaminating products of cellulase digestion (Fig. 2), so it was not further examined. The higher molecular mass subfraction, in contrast, differed in composition between NW and TW (Fig. 5). The proportion of Gal, the major monomer, was considerably higher, while the proportion of Man, the second most abundant monomer and indicative of mannan, was lower in TW samples. The remaining monosaccharides (including Rha and GalA, indicative of RG-I) were present in similar proportions in both wood types (Fig. 2). Interestingly, Man was substantially more abundant than Xyl in the cellulose-retained fraction of both TW and NW, in sharp contrast to the 88:12 Xyl to Man ratio in the KOH extractable fraction (Fig. 5).

The high molecular mass polysaccharides were further characterized by enzyme hydrolysis and PACE analysis. Following the endo-β-(1→4)-galactanase treatment, oligosaccharides co-migrating with Gal, β-(1→4)-galactan dimer and trimer were released from the TW samples. Very small amounts of β-(1→4)-galactooligosaccharides were detected in this fraction from NW (despite loading gels with the same amounts of total sugar as when analyzing TW samples), indicating that extremely little β-(1→4)-galactan is present in this fraction of NW, although it is the major polymer in the corresponding TW fraction (Fig. 5D, green arrowheads). To investigate whether the RG-I backbone was also present in this subfraction, the same amounts of TW and NW polymers were subjected to digestion by RG-I lyase and the digestion products were analyzed by separating charged oligosaccharides on 2-aminoacridone (AMAC) gels (Tryfona et al., 2012). These treatments released and resolved a number of RG-I lyase products with various DPs. Due to the absence of appropriate standards the released oligosaccharides could not be further characterized. However, comparison of the oligosaccharide profiles obtained from NW and TW samples shows that they differed in abundance of some of the released oligosaccharides (Fig. 5D, orange arrowheads). This suggests

that the RG-I branching pattern is modified in TW compared to NW. TW samples yielded considerably more of the analyzed subfraction than NW samples, suggesting that RG-I backbones are considerably more abundant in TW. Type II arabinogalactans were also analyzed by exo-β-(1→3)-galactanase hydrolysis and PACE analysis. To allow direct comparison of NW and TW samples they were adjusted to equalize their Ara contents before this analysis. Higher amounts of AG-II were present in TW relative to NW samples, according to differences in abundance of Gal, (Me)GlcA-Gal, (Me)GlcA-Gal_2 and β-1,6-Gal_2 oligosaccharides (Fig. 5E, red arrowheads). This indicates that the TW subfraction contains more AG-II polysaccharides than the corresponding NW subfraction. Moreover, the proportion of these acidic oligosaccharides was higher in this subfraction of TW than in the buffer-soluble subfraction (compare Fig. 5 and Fig. 3), suggesting that there are structural differences between the AG-II in cellulose-retained and soluble polymer fractions of TW.

To obtain more structural information about the β-(1→4)-galactan that was found to be the most prominent of the high molecular weight polymers in the cellulose-retained fraction of TW, a sample of these polymers was analyzed by NMR spectroscopy. In the anomeric region of the ^{1}H spectrum the most intense signal arose from the H1 of β-D-Gal (4.63 ppm). Signals in the 4.72-5.25 ppm region could result from mannose (Man), rhamnose (Rha) and galacturonic acid (GalA) residues. High-intensity signals in the aliphatic spectral region arose mainly from β-D-Gal. Signals at 4.63 (H1) and 4.16 (H4) ppm indicated that Gal is 1,4-linked. Signals at 1.24 and 1.32 ppm, respectively assigned to methyl groups of 2-Rha and 2,4-Rha, suggest that relative proportions of branched and unbranched Rha were 47% and 53%. The ratio (2.71 to 0.45) of integral intensities of well-separated Gal signal (H4) and signals from the three protons of the methyl group of 2,4-Rha indicates that the average length of the β-(1→4)-Gal chains was approximately 18 monomers.

Immunocytochemical localization of polysaccharides in wood sections identifies polymers of the compound middle lamella, S- and G-layers

The polymers that were biochemically identified as differentially abundant in various fractions of TW and NW were localized in different cell wall layers by immunocytochemistry. Representative patters of labeling are shown in Fig. 6 and Fig. S2. The G-layers of TW fibers were heavily labeled with LM5 antibody, specific for β-(1→4)-galactans, while S-layers of both TW and NW were devoid of this labeling (Fig. 6A and Fig. 6B). Signals from LM5 were also detected in the compound middle lamella in both TW and NW. A similar distribution was observed for RG-I backbone epitopes specifically recognized by the RU2 antibody (Fig. 6C and

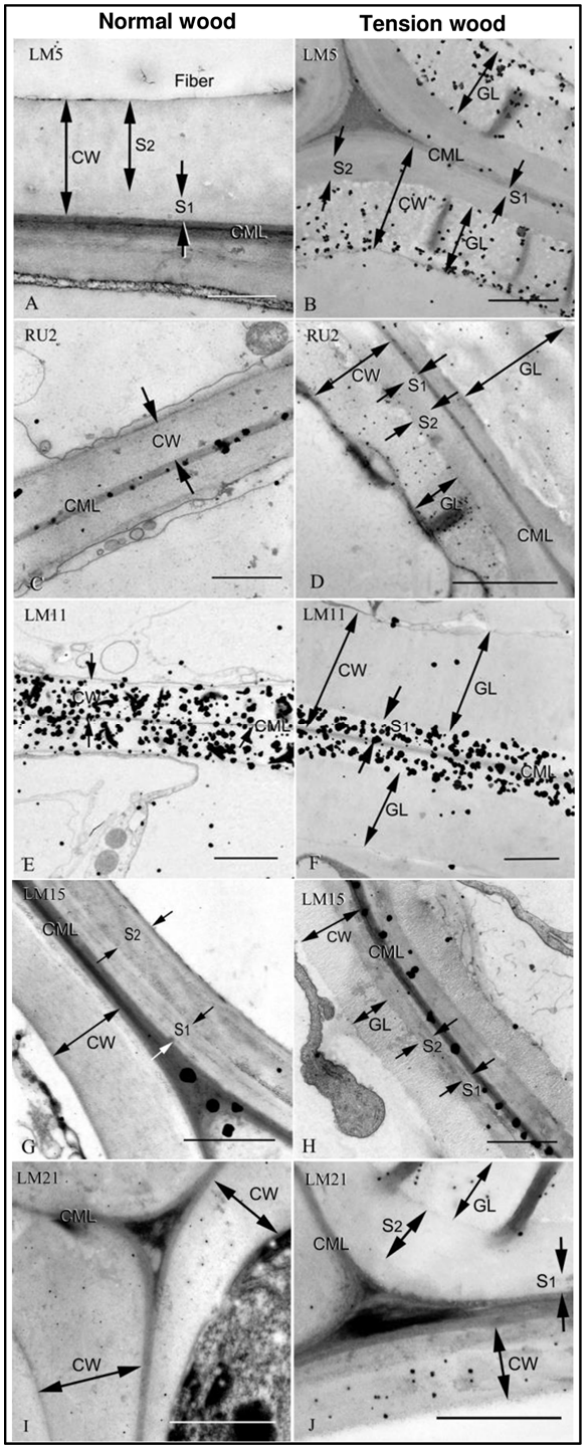

Figure 6. Immunolocalization of cell wall polysaccharides in fibers of normal wood (to the left) and tension wood (to the right) with LM5 antibody (A, B), RU2 antibody (C, D), LM11 antibody (E, F), LM15 antibody (G, H), and LM21 antibody (I, J). CML – compound middle lamella, CW – cell wall, GL – G-layer, S1 and S2 – secondary cell wall layers. Silver enhancement was applied for different times (2-5 min) leading to different sizes of particles. Scale bar: 1.0 μm.

Fig. 6D). A reciprocal label distribution was observed with LM11 antibody, which recognizes β-(1→4)-xylan, as it solely labeled S-layers in both TW and NW fibers (Fig. 6E and Fig. 6F). LM15 revealed XG epitopes in the compound middle lamella, which were more abundant in TW than in NW, and some signals at the S-G boundary and innermost (developing) G-layers in TW fibers (Fig. 6G and Fig. 6H). Attempts to immunolocalize AG-II by electron microscopy were not successful, although signals from the antibodies used were observed in the periplasm of ray parenchyma cells. Similar observations were reported by Lafarguette et al. (2004). We detected

no labeling of fiber cell walls in either TW or NW samples by either the JIM14 antibody, recently classified by multivariate analysis as recognizing AG-II epitopes designated AG-4, or M7 and M22 antibodies classified as recognizing epitopes in RG-I and/or AG-II designated RG-I/AG (Pattathil et al., 2010). LM21, which specifically binds to β-(1→4)- mannans was the only antibody that bound both S-layers in TW and NW and G-layers in TW (Fig. 6I and Fig. 6J). LM21 labeling was weaker in TW S-layers than in TW G-layers and NW S-layers. No labeling was detected in control experiments omitting primary antibodies.

In situ assays reveal higher β-1,4-galactosidase activity in TW than in NW

In gelatinous fibers of flax, the β-(1→4)-galactan is modified by a cell wall GH35 β-galactosidase, which is essential for processing of the high molecular mass galactan and development of a highly crystalline cellulosic cell wall layer (Mikshina, et al., 2009; Roach et al., 2011; Mokshina et al., 2012). We therefore investigated if development of TW also involves β-1,4-galactosidase activity. Freshly prepared TW and NW sections were incubated with Gal-β-resorufin, and the release of resorufin by endogenous β-1,4-galactosidase activity was monitored in real time *in situ*, following Ibatullin et al. (2009) and Banasiak et al. (2014). β-1,4-galactosidase signals were detected in developing NW and TW cell walls and were distinctly stronger in the latter (Fig. 7). In TW samples the signals were most intense in the outer cell wall layers (perhaps the compound middle lamella) and G-layer. No signal was detected in control sections heated before the assay to denature proteins.

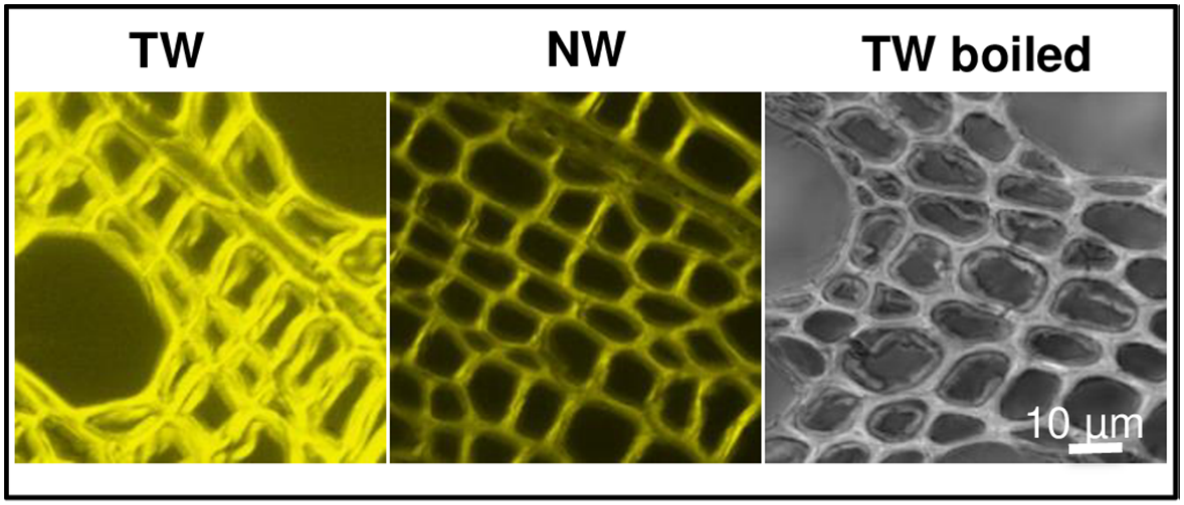

Figure 7. β-1,4-Galactosidase activity is present in cell walls of developing normal wood (NW) and tension wood (TW) and is highly increased in TW. Yellow coloration corresponds to the fluorescence channel signals from resorufin released by the action of β-1,4-galactosidase from the substrate. The control shown on the far right is the image of developing TW that was heated before the assay to denature proteins. No fluorescence signal was detected and the image of the fluorescence channel was superimposed on the transmitted light channel to show the presence of TW tissue.

Discussion

Key differences in the structure and occurrence of matrix cell wall polysaccharides between TW and NW

The major cytological difference between TW and NW in aspen, as in many angiosperms, is the formation of a tertiary gelatinous (G) cell wall layer in TW fibers (Fig. 1). This layer lacks lignin and has very high cellulose contents, cellulose microfibrils oriented parallel to fibers' longitudinal axes, large cellulose crystallites, high mezoporosity, and distinct matrix polysaccharides (reviewed in Mellerowicz and Gorshkova, 2012). Further cytochemical and

biochemical comparisons of matrix cell wall polysaccharides in aspen TW and NW revealed the following similarities and distinctions.

Xylan is by far the major matrix polymer in both TW and NW (Fig. 1 and Fig. 2, Table 1 and Table 2). However, the G-layer in aspen TW does not bind the anti-xylan antibody LM11, which heavily labels S-layers (Fig. 6). Previous assays with several antibodies recognizing secondary wall xylan (LM10, LM11 and AX1) indicate that xylan is also restricted to S-layers in gelatinous TW of several species (Bowling and Vaughn, 2008; 2009; Decou et al., 2009). Sparse labeling of G-layers (relative to S-layers) by LM11 (with no LM10 labeling) in hybrid aspen has been reported (Kim and Daniel, 2012), but Nishikubo et al. (2007) detected no xylan in linkage analysis of isolated G-layers. Thus, exclusion of xylan from the G-layers appears to be the main cause of lower Xyl content in TW (Fig. 1). It also correlates with transcriptomic changes observed following TW induction in aspen, including downregulation of transcripts encoding UDP-xylose synthase, GT8 family members (GT8E, GT8F-1, GT8F-2 – similar to PARVUS, and GT8B-2 – similar to GUX1), and GT47C, all of which are involved in xylan biosynthesis (Andersson-Gunneråas et al., 2006).

Various approaches, including wet chemistry and CCRC-M1 antibody labeling, have demonstrated the presence of XG—the characteristic polysaccharide of primary cell walls, which is absent or reduced in NW S-wall layers (Bourquin et al., 2002)—in G-layers and S2/G boundaries of gelatinous fibers in *Populus* and other species (Nishikubo et al., 2007; Bowling and Vaughn, 2008; Mellerowicz et al., 2008; Baba et al., 2009; Sandquist et al., 2010). Our LM15 labeling confirms its localization in the compound middle lamella, S2/G layer boundaries, and developing G-layers in aspen (Fig. 6). Sequential extraction and size exclusion analyses presented here also show that XG with a low molecular weight (10 kDa) is more abundant in KOH-extractable polymers of TW than in those of NW (Fig. 2 and Fig. 4). Only trace amounts of XG were present in the cellulose-retained polymer fraction in TW (Fig. 2).

The only matrix polymer deposited in both S- and G-layers is β-(1→4)-mannan (Fig. 6I, Fig. 6J). Its presence in isolated G-layers is supported by sugar and linkage analysis (Furuya et al., 1970; Nishikubo et al., 2007). Labeling by LM21 was more prominent in G-layers, as previously reported (Kim and Daniel, 2012). However, Man and mannan contents were lower in TW than in NW (Fig. 1C; Hederström et al., 2009) and transcripts encoding three GDP-Man-pyrophosphorylases, and the putative mannan synthase *Pt*GT2A, are reportedly correspondingly reduced (Andersson-Gunneråas et al., 2006). These findings indicate that mannan levels are reduced in S-layers of TW samples, and LM21 labels S-layers less intensely in TW than in NW (Fig. 6I, Fig. 6J). Interestingly, mannan is one of the main polymers of the cellulose-retained fraction of both NW and TW, but more abundant in NW (Fig. 5). According to previous

451 proposals, the polymer that directly interacts with cellulose in S-layers is mannan in conifers
452 (Åkerholm and Salmén, 2001) and xylan in hardwoods (Salmén and Burgert, 2009), but finding
453 mannan in the cellulose-retained fraction (Fig. 5) suggests that it could also be intimately
454 associated with cellulose in hardwood S-layers.
455 AG-II is a modular polysaccharide of variable structure decorating various AGPs (Tan et
456 al., 2010). Since genes encoding AGPs similar to *AtFLA12* and *AtFLA11* are among the most
457 strongly up-regulated genes following G-layer induction in several species—for examples see
458 Lafarguette et al. (2004), Pilate et al. (2004), Paux et al. (2005), Andersson-Gunnerås et al.
459 (2006) and Roach and Deyholos (2007)—we predicted that specific forms of AG-II would be
460 more abundant in TW compared to NW. An eight-fold increase of the buffer-soluble fraction in
461 TW (Table 1), which is expected to contain most AGPs due to their high water-solubility and
462 proposed periplasmic location (Lamport and Varnai, 2013), and structural differences between
463 buffer-soluble AG-II of TW and NW (Fig. 3), confirmed that specific AGPs are upregulated in
464 TW. These AGPs were not recognized by JIM14, which labeled AG-II in all analyzed fractions
465 more strongly in NW than TW, and KOH-extractable polymers most strongly (Fig. 2). Thus,
466 these JIM14 signals in AG-II probably did not correspond to FLA11- and FLA12-like AGPs. In
467 addition to high abundance in the buffer-soluble fraction, AG-II has been identified as one of the
468 main compounds of cellulose-retained high molecular weight polymers (Fig. 5). Interestingly,
469 this fraction of TW contained significantly more exo-1,3-galactanase-susceptible AG-II, relative
470 to Ara, than the corresponding NW fraction, suggesting that β-(1→3)-galactan specifically
471 expands in TW. Moreover, both buffer-soluble and cellulose-retained AG-II polymers of TW
472 were more acidic than those of NW (Fig. 3D and Fig. 5E). Acidic forms of AGP could play
473 more than a structural role in TW. GlcA of AG-II may be involved in stoichiometric binding of
474 Ca^{2+} (Lamport and Varnai, 2013), which plays key roles in plant signaling pathways (Kudla et
475 al., 2010). Thus, our data imply that Ca^{2+} associated with special acidic AG-II may participate in
476 TW development.
477 Our data also clearly show that higher abundance of RG-I backbone and long β-(1→4)-
478 galactan chains are the main biochemical features distinguishing TW from NW (Fig. 2, Fig. 3
479 and Fig. 5, Table 2). Higher proportions of Gal have been detected in TW than in NW of several
480 species (Meier, 1962; Kuo and Timmel, 1969; Furuya et al., 1970; Ruel and Barnoud, 1978;
481 Mizrachi et al., 2014) and β-(1→4)-galactan has been detected in G-layers of aspen (Arend,
482 2008). However, β-(1→4)-galactan has not been previously shown to co-occur with RG-I in
483 TW. We detected RG-I backbone and β-(1→4)-galactan signals from RU2 and LM5 antibodies,
484 respectively, in the compound middle lamella and G-layer (Fig. 6). We also detected RG-I

485 backbone and β-(1→4)-galactan in all polysaccharide fractions of TW (Fig. 2, Fig. 5), including
486 polymers retained in cell walls so tightly that they can be extracted only after dissolution of
487 cellulose microfibrils. In lignified cell walls a polysaccharide may remain unextractable by
488 strong alkali if it is linked to lignin, but as there is virtually no lignin in G-layers (Love et al.,
489 1994, Gorshkova et al., 2000; Kaku et al., 2009), the RG-I with β-(1 → 4)-galactan,
490 immunolocalized in G-layers, could only remain unextracted if trapped between cellulose
491 microfibrils.
492
493 ***Differences and similarities between flax and aspen gelatinous fibers***
494 As in flax fibers, RG-I backbone is present, together with β-(1→4)-galactan chains, in the
495 polymers retained in TW by cellulose microfibrils. The structure of the TW RG-I co-extracting
496 with β-(1→4)-galactan resembles that of flax phloem fibers: according to NMR analysis
497 presented here and by Mikshina et al. (2012) the degree of RG-I backbone substitution is 50% in
498 aspen and 30% in flax phloem, and the average length of β-(1→4)-Gal chains in these species is
499 18 and 14, respectively. Although we have not demonstrated the linkage between Rha and Gal
500 in aspen, it has been fully resolved in flax (Mikshina et al., 2012; 2014). Flax fiber RG-I
501 molecules can form water-soluble complexes having β-(1→4)-galactan chains in the center and
502 acidic RG-I backbones at the periphery (Mikshina et al., 2015). Structural similarities suggest
503 that the aspen TW counterpart also has such ability. Acidic AG-II, detected in the cellulose-
504 retained fraction of aspen TW, has not been characterized to date in flax fibers. However, strong
505 upregulation of FLA11- and FLA12-like AGPs during flax fiber development (Roach and
506 Deyholos 2007) suggests that this form of AG-II is also present in flax. The relationship
507 between AG-II and RG-I—both of which are potential sources of carboxylic acid residues
508 observed by dynamic FTIR spectroscopy in aspen TW (Olsson et al., 2011)—remains to be
509 determined.
510 In flax, mature G-layers form from initially deposited Gn-layers, which can be clearly
511 distinguished in electron micrographs (Gorshkova et al., 2004, 2010). The maturation involves
512 post-deposition modification of nascent RG-I galactan by the galactosidase *Lu*BGAL1 (Mikshina
513 et al., 2009; Roach et al., 2011; Mokshina et al., 2012), and is essential for flax stems'
514 mechanical properties (Roach et al., 2011). The Gn structure is not pronounced in TW fibers,
515 but many studies have detected an inner G-layer with different properties from the rest
516 (Lafarguette et al., 2004; Joseleau et al., 2004; Gerlinger and Schwanninger, 2006). Moreover,
517 *we* detected high β-galactosidase activity in developing TW fibers (Fig. 7), and a flax-specific
518 galactosidase epitope has been detected in the G-layer of aspen TW (Mokshina et al., 2012),

519 strongly suggesting involvement of a homologous galactosidase in pectic β-(1→4)-galactan
520 processing in TW.
521 The key difference in cell wall organization between gelatinous phloic fibers of flax and
522 gelatinous xylary fibers of aspen concerns the degree of S-layer development. The flax S-layer
523 is difficult to discern even in electron micrographs (Andème-Onzighi et al., 2000; Salnikov et al.,
524 2008), but can be revealed by labeling with xylan-specific antibodies (Gorshkova et al., 2010).
525 Thus, both types of gelatinous fibers have the same general type of cell wall architecture with
526 primary, secondary and tertiary walls. Aspen TW fibers, as in other tree species, always have at
527 least one well-developed S-layer (Fagerstedt et al., 2014) characterized by the presence of xylan
528 and helicoidal orientation of cellulose microfibrils with high cellulose microfibril angles (Clair et
529 al., 2011; Rüggeberg et al., 2013). A xylan layer with nearly transversal cellulose orientation is
530 probably required for its resistance to radial compression, which is poor in the G-layer with axial
531 cellulose orientation. In herbaceous plants the mechanical forces acting on developing phloem
532 fibers in radial direction (and hence the need for S-layers) may be weaker than in wood.
533 Thus, although flax and aspen are sufficiently closely related to belong to the same order
534 (Malpighiales), they develop gelatinous fibers in different tissues and of different origin (in
535 primary phloem initiated from the procambium and in secondary xylem produced by the vascular
536 cambium, respectively). The structural similarities of these fibers suggest that other contractile
537 cell walls with G-layers may also have similar structures and properties.
538

539 ***Implications of the findings for the entrapment-based TW contraction hypothesis***

540 TW plays a key physiological role in maintaining stems and branches with secondary
541 growth in appropriate positions by generating tensional longitudinal stress. Characteristic
542 contractile properties of TW with gelatinous fibers are known to originate from the G-layers
543 (Clair and Thibaut 2001; Yamamoto et al., 2005; Clair et al., 2006; Fang et al., 2008) that are
544 firmly attached to S-layers in their native state (Clair et al, 2005), possibly through XG cross-
545 links (Nishikubo et al., 2007; Bowling and Voughn, 2008; Sandquist et al., 2010). The G-layers
546 were long assumed to consist almost entirely of cellulose (Norberg and Meier 1966).
547 Consequently, hypotheses regarding the origin of tension were based on cellulose microfibrils'
548 arrangements (Burgert and Fratzl, 2009). All microfibrils in thick G-layers lie almost parallel to
549 each other and the longitudinal cell axis, in sharp contrast to the helicoidal arrangement of
550 microfibrils in secondary cell wall layers (Rüggeberg et al., 2013; Fagerstedt et al., 2014). The
551 difference in microfibril orientation provides the basis for pine cone opening and wheat awn
552 movement mechanisms (Burgert and Fratzl, 2009), and may be involved in creation of tension in

553 TW (Goswami et al., 2008). However, this mechanism is highly dependent on air humidity and
554 the movement is reversible, which is not the case in TW. Thus, additional factors must influence
555 tension creation involving G-layers.
556 Re-discovery of the significant content of matrix polysaccharides in the G-layer (reviewed
557 in Mellerowicz and Gorshkova, 2012; Fagerstedt et al., 2014) increased attention to their
558 possible role in tension generation (Fournier et al., 2014). Recent evidence shows that cellulose
559 crystallites of the G-layers have larger lattice spacing than corresponding crystallites of the S-
560 layers in NW, and this difference appears as the G-layer is deposited (Clair et al., 2011). The
561 spacing is reduced as the tension stress is released and its reduction corresponds exactly to
562 macroscopic strain at the stem surface, indicating that cellulose fibrils are under tension in TW
563 (Clair et al., 2006). We previously suggested that the tension could arise during microfibril
564 lateral interaction with entrapment of matrix polysaccharides (Mellerowicz et al., 2008,
565 Mellerowicz and Gorshkova 2012). With low matrix polysaccharide contents and no lignin,
566 microfibril lateral contacts are frequent in the G-layer, leading to the formation of macrofibrils
567 and explaining its high crystallinity (Müller et al., 2006; Yamamoto et al., 2009). However,
568 entrapment of polysaccharides between cellulose microfibrils would limit their interaction and
569 force them to bend around these polymers, thereby increasing the longitudinal lattice distance
570 stretching the microfibrils and creating tension in them (Mellerowicz et al., 2008, Mellerowicz
571 and Gorshkova 2012).
572 The present work identified polymers trapped within cellulose fibrils in TW of hybrid
573 aspen as RG-I with β-(1→4)-galactan accompanied by a specific acidic form of AG-II.
574 Conditions for lateral interaction of cellulose microfibrils in TW may be provided *in muro* by
575 trimming of the deposited galactans by fiber-specific galactosidases (Roach et al., 2011,
576 Mokshina et al., 2012; Fig. 7). A gelatinous fiber model consistent with these new data is
577 presented in Fig. 8. RG-I with β-(1→4)-galactan is thought to form water-soluble
578 supramolecular structures with low affinity to cellulose (Mikshina et al., 2015). The high
579 hygroscopicity of RG-I (and possibly acidic AG-II) would retain water in the G-layer (Schreiber
580 et al., 2010), accounting for these layers' gel-like properties and their collapse during TW drying
581 (Clair et al., 2006; Clair et al., 2008). Pockets containing these hydrated polymers could also
582 explain the characteristically high mesoporosity of G-layers (Clair et al., 2008; Chang et al.,
583 2009; 2015). Mesopores of various sizes (2-60 nm) and shapes (ink bottle and slit-like)
584 reportedly form during G-layer deposition (Chang et al., 2015), correlating with tensional stress
585 development (Clair et al., 2011). Thus, hydrated galactans identified in this study as cellulose-
586 retained polymers could provide the contractile driving force in TW G-layers.
587

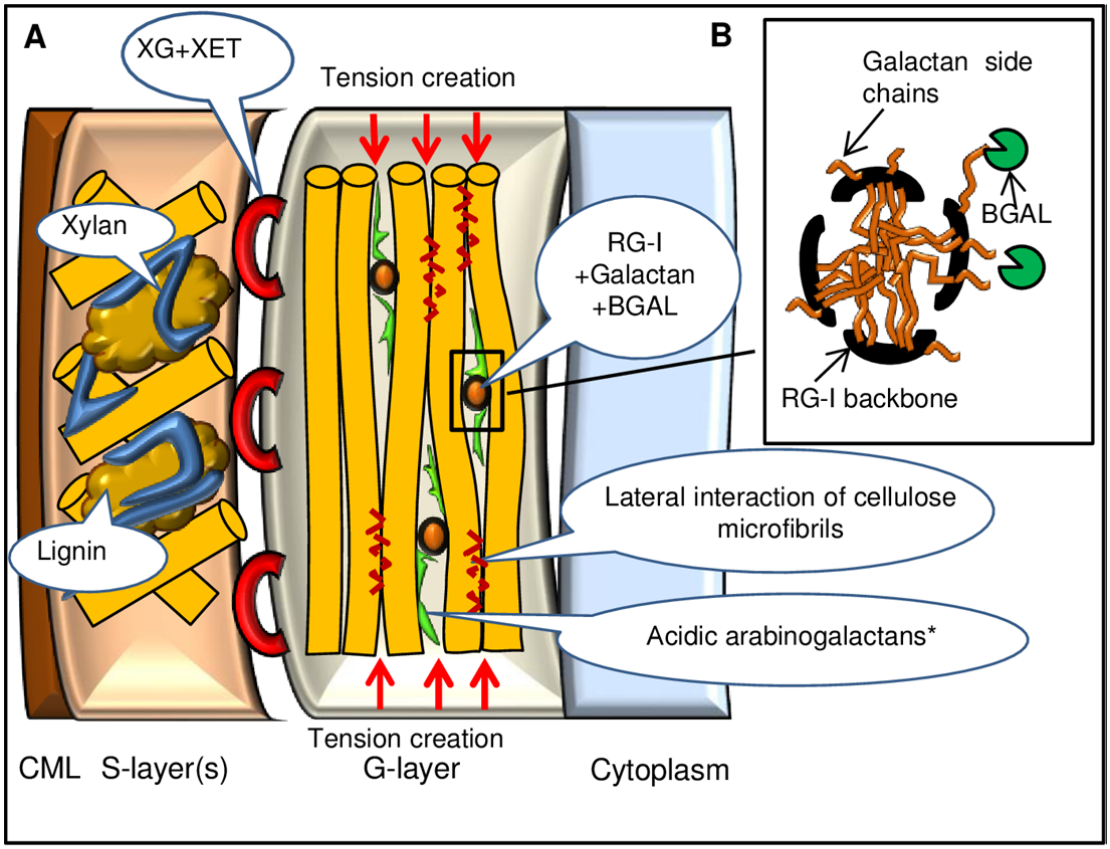

Figure 8. A, A scheme of the main components in S and G cell wall layers of fibers in tension wood. In S-layers, cellulose microfibrils are oriented helicoidally with alternating MFA between layers; in thick G-layers the orientation of all cellulose microfibrils is close to axial. XG+XET – xyloglucan and xyloglucan endotransglycosylase, which acts to staple S- and G-layers (Mellerowicz et al., 2008; Hayashi et al., 2010). Cellulose microfibrils in S-layers are separated by xylan and lignin, and have poor chances to interact laterally; in highly cellulosic G-layers microfibrils tend to interact laterally, thereby increasing crystallinity. RG-I+Galactan – rhamnogalacturonan I and β-(1→4)-galactan trapped between laterally interacting G-layer cellulose microfibrils, creating tension in them. Galactan chains are modified *in muro* by specific galactosidase (BGAL), making the polymer more compact and providing conditions for lateral interaction of cellulose microfibrils (not shown). CML – compound middle lamellae. **B,** Possible spatial structure of the RG-I and galactan (Mikshina et al., 2015): β-(1→4)-galactan side chains (galactan) attached to RG-I backbone; molecules of RG-I are associated due to β-(1→4)-galactan chain interaction, note the backbone is located at the surface of such associated molecules.

Materials and Methods

Plant material

590 Rooted cuttings of hybrid aspen (*Populus tremula* L. × *tremuloides* Michx.), clone T89,
591 were grown in a greenhouse at 20° C and 60% relative humidity with an 18 hr photoperiod and
592 supplementary lighting (Osram Powerstar HQI-BT 400 W/D, Osram, Germany) switched on
593 when the incoming light fell below 20 W/m^2 during the photoperiod. Plants were watered daily
594 and fertilized with a complete nutrient solution (SuperbaS, Supra HydrO AB, Landskrona,
595 Sweden) once a week. To induce TW, five one-month old plants were tilted at 45 degrees from
596 vertical with their basal stem parts secured to tilted stakes, at approximately 1 m from the base,
597 and they were grown in this position for approximately six weeks. Control trees were grown in
598 upright position with their stems secured to vertical stakes. Approximately 1 m of the basal part
599 of the stem from both tilted and upright trees was harvested, frozen in liquid nitrogen and kept at
600 -20° C until analysis. TW produced by the tilted trees, and NW produced by the upright trees,
601 was dissected from stem segments and freeze-dried, ground in a ZM 200 centrifugal mill (Retsch
602 GmbH, Haan, Germany) at 14 000 rpm and in each case the resulting powder was passed
603 through a sieve with 0.5 mm mesh.
604
605 ***Cell wall isolation and fractionation***
606 Portions of the powdered TW and NW samples (1 g for each replicate) were
607 homogenized on ice in 30 ml of 50 mM KH_2PO_4-NaOH buffer, pH 7.0. After centrifugation of
608 each homogenate (8000 g, 25 min), the supernatant was filtered and incubated for 15 min in a
609 boiling water bath to inactivate endogenous enzymes. The supernatant was then cooled, ethanol
610 was added to 80% (v/v) and the mixture was incubated overnight at 4°C to precipitate the buffer-
611 extractable polysaccharides. The resulting pellet was washed three times with 80% ethanol and
612 once with 80% acetone then dried.
613 Cell wall material from each pellet obtained after homogenization was isolated according
614 to Talmage et al. (1973). Briefly, it was sequentially washed with water (3x), 80% ethanol,
615 acetone (overnight, 4°C), water (3x) and 50 mM KH_2PO_4-NaOH buffer (pH 7.0) (2x), digested
616 overnight with 2 mg/ml glucoamylase supplied by Siekagaki Kogyo (Rockville, MD), washed
617 with the same phosphate buffer, water (3x), and acetone then dried.
618 Cell wall polymers were extracted sequentially by 1% ammonium oxalate (AO) (pH 5.0,
619 boiling water bath, 1 h) and after washing with water by 4 M KOH with 3% H_3BO_4 (2 h). The
620 KOH fractions were neutralized by adding acetic acid to pH 7.0. Fractions extracted by
621 ammonium oxalate and alkali were desalted by passage through a Sephadex G‐25 column
622 (19×400 mm) and dried.

The residue remaining after AO and KOH treatment was washed by water and dried. A 2 mg portion was hydrolyzed by incubation with 2M TFA at 120°C for 1 h to determine its sugar content by monosaccharide analysis. The rest of the pellet was used to isolate matrix polysaccharides in polymeric form, following Gurjanov et al. (2008). Briefly, it was dissolved in 8% LiCl in N,N-dimethylacetamide (DMA), cellulose was precipitated by water and degraded by incubation with 1% Cellusoft-L cellulase (Novo Nordisk Bioindustrie S.A., Paris, France; 750 EGU/G) in 10 mM NaOAc buffer, pH 5.2, at 33ºC overnight. Supernatants obtained after dissolution with LiCl in DMA and cellulose degradation were concentrated by partial lyophylization, separated from salts and low-molecular weight products of cellulose digestion by passage through a Sephadex G-25 column (19×400 mm), combined and dried. The resulting fraction was designated cellulose-retained polymers.

The pellet remaining after partial removal of KOH-unextractable matrix polymers and cellulose digestion was washed by water, dried, hydrolyzed by 2M TFA and subjected to monosaccharide analysis (to obtain "lignin-bound polymers"). The difference between the pellet dry mass and total monosaccharide yield was designated the "lignin content". The fractionation procedure is summarized in Fig. S1.

"Cellulose" content was calculated by subtracting yields of all obtained fractions (buffer-extractable, AO-extractable, KOH-extractable, KOH-unextractable polymers, and lignin) from the dry mass of the initial sample.

Gel-filtration by HPLC

The obtained fractions of matrix polysaccharides were dissolved in 0.2 M Na_2HPO_4 with 0.05% of NaN_3, pH 6.8. Aliquots were taken for sugar content determination by phenol-sulphuric acid method (Dubois at al., 1956), for monosaccharide analysis and for immunodot analysis of total fractions. 500-1000 μg portions of the obtained fractions were size-fractionated in the same buffer by an HPLC system (Gilson, France) equipped with combined G5000PW and G4000PW TSKgel columns (Tosoh Bioscience, Japan). Calibration was performed using Dextran (2000 kD, Sigma), pullulan standards with molecule weights 1600, 400, 200, 100, 50, 10, 5 kDa (Waters) and Gal (0.18 kD, Merck). To obtain elution profile after gel-filtration, 0.6 ml probes were collected and total sugars were quantified in each probe by the phenol-sulfuric acid method (Dubois et al., 1956) using Glc (Merck) as a standard. The presented elution profiles are means obtained from three independent biological replicates based on the carbohydrate contents of the probes and total amounts of sugar in the fractions.

According to the two major peaks in the elution profiles, buffer-soluble, KOH-extractable and cellulose-retained polymers were each subdivided into two subfractions. Corresponding probes were combined, desalted by passage through a Sephadex G-25 column (15x50 mm), and concentrated using a vacuum evaporator. Portions of these preparations were used for monosaccharide determination, and (when applied) immunochemical characterization or enzymatic hydrolysis with PACE analysis.

Monosaccharide analysis

Samples for monosaccharide analysis were dried, hydrolyzed with 2 M TFA at 120°C for 1 h, dried to remove TFA, dissolved in water and analyzed by high-performance anion exchange chromatography using an DX-500 instrument equipped with a 4x250 mm CarboPac PA-1 column and a pulsed amperometric detector (all from Dionex, USA). The column temperature was 30°C and the mobile phase (pumped at 1 ml/min) consisted of 100% B (0-20 min), 90% B (20-21 min), 50% B (22-41) min, 0% B (42-55 min), and finally 100% B (56-85 min), where B was 15 mM NaOH, and the other solvent (A) was 100 mM NaOH in 1 M sodium acetate. In some additional experiments Xyl and Man were separated by isocratic elution with 1.8 mM NaOH buffer. The results were analyzed using PeakNet software according to the calibrations obtained for monosaccharide standards treated in advance with 2 M TFA at 120ºC, 1 h. Three independent biological replicates and two analytical replicates of NW and TW samples were analyzed.

Immunodot analysis

Total fractions or subfractions containing 4, 1, and 0.25 µg of sugar (1-3 µl) were applied to nitrocellulose membranes (0.2 µm, Sigma). Membranes were air-dried for 30 min, washed for 5 min in PBST (phosphate-buffered saline with 0.05% Triton X-100), blocked for 1 h with PBS containing 3% of nonfat dry milk (PBS/milk), then incubated for 40 min with primary monoclonal antibody. The monoclonal antibodies used were: LM5 (Jones et al., 1997), LM11 (McCartney et al., 2005), LM15 (Marcus et al., 2008), LM21 (Marcus et al., 2010), JIM14 (Knox et al., 1991), and RU2 (Ralet et al., 2010), all raised in rat except RU2 (mouse, hybridoma supernatant). They are respectively specific for β-(1→4)-galactan, β-(1→4)-xylan, the XXXG motif of XG, β-(1→4)-mannan, an unknown epitope of AGP and rhamnogalacturonan I backbone. The antibodies were kindly provided by Prof. P.Knox (University of Leeds, UK) (LM5, LM11, LM15, LM21, JIM14) and Dr. F. Guillon (INRA, Nantes, France) (RU2). LM5, LM11, LM15, LM21, JIM14 were applied at 1:30 dilution, and RU2 at 1:10 dilution, in PBST.

690 After incubation with primary antibodies, membranes were washed three times for 10 min with
691 PBST then incubated with secondary biotinylated antibodies (Sigma) (anti-rat to detect LM5,
692 LM15, LM11, LM21, JIM14 primary antibodies, and anti-mouse to detect RU21) for 40 min.
693 The membranes were washed again three times in PBST for 10 min, incubated for 30 min in
694 streptovidin conjugated with alkaline phosphatase diluted 1:3000 and developed using a
695 nitroblue tetrazolium/5-bromo-4-chloro-3-indolyl phosphate kit (Silex). Potato galactan and
696 rhamnogalacturonan I, arabinoxylan from wheat flour and XG from tamarind seeds (all supplied
697 by Megazyme) were used as positive controls.
698

699 ***Enzymatic hydrolysis and PACE analysis***

700 For β-(1→4)-galactan analysis, subfractions of interest with equal amounts of total sugars
701 were digested by incubation with endo-β-(1→4)-galactanase in 10 mM ammonium acetate, pH
702 6.0, at 37˚C for 24 h. β-(1→4)-Galactan standards were prepared from lupin seed pectic
703 galactan (Megazyme) by endo-β-(1→4)-galactanase hydrolysis. For treatment with RG-I lyase
704 prepared from *Aspergillus aculeatus* (Jensen et al., 2010), samples adjusted to equal amount of
705 total sugar were dissolved in 500 µl of 0.05 M Tris-HCl solution, pH 8.0, containing 2 mM
706 $CaCl_2$ and incubated at 21°C for 24 h. For type II arabinogalactan analysis, samples were
707 adjusted to equal amounts of total Ara and hydrolysed by AG-specific enzymes as described by
708 Tryfona et al. (2012). Carbohydrates were derivatized, electrophoretically separated and
709 subjected to PACE gel scanning and quantification as described by Goubet et al. (2002, 2009).
710 Neutral fragments were separated on 8-aminonaphthalene-l,3,6-trisulfonic acid (ANTS) gels, and
711 acidic fragments on AMAC gels. The identity of digestion products was established by mass
712 spectrometry in a previous study (Tryfona et al., 2012). Control experiments without substrates
713 or enzymes were performed under the same conditions to detect non-specific compounds
714 potentially present in the enzyme preparations, polysaccharides/cell walls or labelling reagents.
715

716 ***Transmission electron microscopy and immunocytochemistry***

717 Segments (ca. 5 mm x 5 mm x 15 mm in tangential, radial, and longitudinal directions,
718 respectively) containing developing TW and NW were cut from the stem of tilted (Fig. 1) and
719 upright trees, put immediately in 4% paraformaldehyde + 0.5% glutaraldehyde in 0.05 M Na-
720 phosphate buffer (pH 7.4), cut into 2.0 mm x 3.0 mm x 5.0 mm pieces and infiltrated under
721 vacuum for 5 min. Then samples were cut into smaller (1.5 mm x 1.5 mm x 2.5 mm) pieces, left
722 in fresh portions of the same buffer for 3 h at room temperature and post-fixed with 0.5% OsO_4
723 in 0.1 M Na-phosphate buffer (pH 7.4) for 4 h. After dehydration, the samples were embedded

724 in LR White resin (Medium Grade Acrylic Resin, Ted Pella Inc., Cat. No. 18181). Ultrathin
725 sections were cut with a diamond knife and LKB Ultracut III ultramicrotome (Sweden) then
726 mounted on Formvar-coated 100-mesh nickel grids. For immunolocalization, thin sections on
727 nickel grids were blocked (15 min, RT, in a high humidity chamber) in TBST (Tris-Buffered
728 Saline, 0.02 M, pH 7.5 and 0.1% Tween 20) plus 5% goat serum (Sigma 5-2007), and incubated
729 for 1–1.5 h at room temperature with LM5, LM11, LM21 or RU2 primary antibody (for
730 information on antibodies see above). LM5, LM11 and LM21 antibodies were used at 1:200
731 dilution in TBST/5% normal goat serum, while RU2 antibody was used without dilution. After
732 incubation with each antibody the samples were washed three times in 0.02 M Tris-buffer, pH
733 8.2, with 0.02% azide, incubated in secondary antibody (1:50 goat anti-rat for LM5 and LM11,
734 and 1:50 goat anti-mouse for RU2) coupled in both cases to 5 nm colloidal gold (Amersham
735 Pharmacia Biotech, Piscataway, NJ) in TB plus 0.06% BSA for 1–1.5 h at room temperature,
736 then washed in TB and H_2O. A BBInternational Silver Enhancing Kit (Ted Pella Inc, Redding,
737 CA) was used to enhance signals of gold particles conjugated with secondary antibody. The
738 solution was applied for 2-5 minutes (Hainfeld and Powell 2000). Sections were stained for 20
739 min with 2% aqueous uranyl acetate and then for 2 min with lead citrate at room temperature
740 (Reynolds 1963, Bozzola and Russell, 1999). Primary antibodies were omitted in control
741 experiments. Sections were observed and photographed using a 1200 EX transmission electron
742 microscope (Jeol, Japan) operating at 80 kV.
743

744 ***NMR spectroscopy***

745 Polymers obtained after cellulose dissolution were dissolved in D_2O (99.9%, Ferak,
746 Germany), dried, then re-dissolved in D_2O (99.994%, Aldrich, USA). ^1H spectra were recorded
747 at 303 K using a Bruker AVANCE III NMR spectrometer (Bruker, Germany) operating at 600
748 MHz. The acquired data were processed and analyzed using Topspin 2.1 software (Bruker,
749 Germany).
750

751 ***In situ β-galactosidase activity***

752 The substrate for β-1,4-galactosidase, resorufinyl-4-*O*-(β-D-Galactopyranoside) (Gal-β-
753 Res), synthesized as described by Ibatullin et al. (2009), was a kind gift from Dr. Harry Brumer.
754 Free-hand TW and NW sections were placed in assay buffer containing 47 mM Gal-β-Res and
755 25mM 2-morpholino-ethanesulfonic acid (MES) at pH 6.5 and the evolution of the fluorescent
756 signal from resorufin was monitored by time-lapse confocal microscopy during 80 min, using an
757 LSM 510 instrument (Carl Zeiss). The presented micrographs were taken when the signal

plateaued, after 20 min. The argon-krypton laser line at 568 nm excitation and over 570 nm emission was used. Signals from the transmitted light channel and fluorescence channels were recorded separately. Control sections were heated at 95°C in the MES buffer for 30 min prior to incubation with the substrate, using the same scanning conditions as for experimental sections.

Acknowledgements

We thank Dr. H. Brumer (University of British Columbia, Canada) for Gal-β-resorufin, and both Prof. P. Knox (University of Leeds, UK) and Dr. F. Guillon (INRA, Nantes, France) for the antibodies.

Figure captions

Figure 1. Anatomy (A), macroscopic appearance (B) and monosaccharide composition (C) of normal and tension wood. **A,** Light microscopy images of normal wood from an upright tree and tension wood from a tilted tree stained with alcian blue-safranin. Note the prominent non-lignified G-layers stained blue in tension wood, and lignified compound middle lamella and S layers stained red in both normal and tension wood. Bar = 50 μm. **B,** Appearance of normal and tension wood after milling. **C,** Monosaccharide composition (mol %) of TFA hydrolyzates of normal and tension wood.

Figure 2. Immunodot analysis of cell wall polysaccharides in buffer-extractable, KOH-extractable and cellulose-retained (obtained after cellulase treatment) fractions of normal and tension wood (NW and TW, respectively) with antibodies recognizing: (1→4)-β-xylan (LM11) (McCartney et al., 2005), (1→4)-β-galactan (LM5) (Jones et al.1997), rhamnogalacturonan I backbone (RU2) (Ralet et al., 2010), the XXXG motif of xyloglucan (LM15) (Marcus et al., 2008), and an unknown epitope of arabinogalactan protein (JIM14) (Knox et al., 1991). Total fractions (aliquots taken before gel-filtration) were used for analysis. 4 μg, 1 μg and 0.25 μg on top of the membrane images indicate the amount of carbohydrates spotted on each vertical line of dots.

Figure 3. Analysis of two subfractions of buffer-extractable polysaccharides of normal and tension wood (NW and TW, respectively). **A,** Elution profile with designation of two subfractions. **B and C,** Proportions of monosaccharides obtained after TFA hydrolysis of high and low molecular weight fractions, respectively. **D and E,** Oligosaccharide fragments obtained after enzymatic digestion and separation by PACE on ANTS gels. For the type II arabinogalactan analysis, the high molecular mass subfractions of NW and TW were adjusted to equalize their total Ara contents and digested with exo-β-(1→3)-galactanase alone or in combination with arabinofuranosidase (D). For β-(1→4)-galactan analysis, the same samples were adjusted to equalize total sugar amounts and digested with endo-β-(1→4)-galactanase (E). Controls are the samples without enzymatic digestion to check for background signals. Bands with differing yields from NW and TW samples are marked by arrowheads: (red) - released with exo-β-(1→3)-galactanase, (blue) - by α-arabinanase followed by exo-β-(1→3)-galactanase, and (green) – by endo-β-(1→4)-galactanase. Error bars in graphs B and C show the standard error of the mean, n=3 biological repeats.

Figure 4. Analysis of two subfractions of KOH-extractable cell wall polysaccharides of normal and tension wood (NW and TW, respectively). **A,** Elution profile with designation of two subfractions. **B and C,** Proportions of monosaccharides obtained after TFA hydrolysis of high and low molecular weight fractions, respectively. **D,** Immunodot analysis of the subfractions with antibodies recognizing (1→4)-β-xylan (LM11) (McCartney et al., 2005), (1→4)-β-galactan (LM5) (Jones et al. 1997), rhamnogalacturonan I backbone (RU2) (Ralet et al., 2010), (1→4)-β-mannan (LM21) (Marcus et al., 2010), and the XXXG motif of xyloglucan (LM15) (Marcus et al., 2008). 4 µg, 1 µg and 0.25 µg on top of the membranes indicate the amount of carbohydrates spotted on each vertical line of dots. Error bars in graphs B and C show the standard error of the mean, n=3 biological repeats.

Figure 5. Analysis of two subfractions of cellulose-retained polymers from samples of normal and tension wood (NW and TW, respectively). **A,** Elution profile with designation of two subfractions. **B and C,** Proportion of monosaccharides obtained after TFA hydrolysis of high and low molecular weight fraction, respectively. **D and E,** Oligosaccharide fragments obtained after enzymatic digestion and separation by PACE on ANTS or AMAC gels. For the β-(1→4)-galactan, the high molecular mass subfractions of NW and TW were adjusted to equalize total sugar amounts and digested with endo-β-(1→4)-galactanase (D). For the RG-I backbone treatment experiments (Jensen et al., 2010), similar samples were digested with RG-I lyase (D). No standards were available for the RG-I fragments. For the type II arabinogalactan analysis, the high molecular mass subfractions of NW and TW were adjusted to equalize amounts of total Ara and digested with exo-β-(1→3)-galactanase (E). Controls are the samples without enzymatic digestion to check for background signals. Bands with differing yields from NW and TW are marked by arrowheads: (green) – released with endo-β-(1→4)-galactanase, (red) – released with exo-β-(1→3)-galactanase, (orange) – released by RG-I lyase. Error bars in graphs B and C show the standard error of the mean, n=3 biological repeats.

Figure 6. Immunolocalization of cell wall polysaccharides in fibers of normal wood (to the left) and tension wood (to the right) with LM5 antibody (A, B), RU2 antibody (C, D), LM11 antibody (E, F), LM15 antibody (G, H), and LM21 antibody (I, J). CML – compound middle lamella, CW – cell wall, GL – G-layer, S1 and S2 – secondary cell wall layers. Silver enhancement was applied for different times (2-5 min) leading to different sizes of particles. Scale bar: 1.0 µm.

Figure 7. β-1,4-Galactosidase activity is present in cell walls of developing normal wood (NW) and tension wood (TW) and is highly increased in TW. Yellow coloration corresponds to the fluorescence channel signals from resorufin released by the action of β-1,4-galactosidase from the substrate. The control shown on the far right is the image of developing TW that was heated before the assay to denature proteins. No fluorescence signal was detected and the image of the fluorescence channel was superimposed on the transmitted light channel to show the presence of TW tissue.

Figure 8. A, A scheme of the main components in S and G cell wall layers of fibers in tension wood. In S-layers, cellulose microfibrils are oriented helicoidally with alternating MFA between layers; in thick G-layers the orientation of all cellulose microfibrils is close to axial. XG+XET – xyloglucan and xyloglucan endotransglycosylase, which acts to staple S- and G-layers (Mellerowicz et al., 2008; Hayashi et al., 2010). Cellulose microfibrils in S-layers are separated by xylan and lignin, and have poor chances to interact laterally; in highly cellulosic G-layers microfibrils tend to interact laterally, thereby increasing crystallinity. RG-I+Galactan – rhamnogalacturonan I and β-(1→4)-galactan trapped between laterally interacting G-layer cellulose microfibrils, creating tension in them. Galactan chains are modified *in muro* by specific galactosidase (BGAL), making the polymer more compact and providing conditions for lateral interaction of cellulose microfibrils (not shown). CML – compound middle lamellae. **B,** Possible spatial structure of the RG-I and galactan (Mikshina et al., 2015): β-(1→4)-galactan side chains (galactan) attached to RG-I backbone; molecules of RG-I are associated due to β-(1→4)-galactan chain interaction, note the backbone is located at the surface of such associated molecules.

Tables

Table 1. Yields of indicated cell wall fractions (mg/g DW of wood) in normal wood (NW) and tension wood (TW). Data are means ± *SE, n*=3.

Fraction	**NW**, mg/g DW	**TW**, mg/g DW
Buffer-extractable polymers[a]	1±0	8±1
AO-extractable polymers[a]	3±0	2±0
KOH-extractable polymers[a]	217±22	126±14
KOH-unextractable (hydrolysable by TFA, w/o Glc)[b]	19±3	25±7
Lignin[c]	211±16	109±12
"Cellulose"[d]	549±20	730±26

[a] determined as sugar content by the phenol-sulfuric acid method (Dubois et al., 1956);
[b] determined as the sum of yields of all monosaccharides obtained by TFA hydrolysis from the pellet remaining after AO and KOH treatments;
[c] calculated by subtracting yields of all monosaccharides obtained by TFA hydrolysis from the pellet remaining after removal of KOH-unextractable matrix polymers and cellulose;
[d] calculated from the dry mass of the initial sample by subtracting yields of buffer-extractable, AO-extractable, KOH-extractable, KOH-unextractable polysaccharides and lignin.

Table 2. Proportions (mol %) and yields (mg/g DW of wood) of monosaccharides in indicated fractions of tension and normal wood (TW and NW, respectively). Data are means ± *SE, n*=3 biological repeats

Fraction	Rha		Ara		Gal		Glc		Xyl(Man)		GalA		GlcA	
	NW	**TW**	**NW**	**TW**	**NW**	**TW**	**NW**	**TW**	**NW**	**TW**	**NW**	**TW**	**NW**	**TW**
mol %														
Buffer-extractable polymers	**9±2**	**13±1**	8±2	5±2	**30±3**	**51±4**	10±5	2±1	**24±8**	**2±0**	**17±3**	**27±2**	**3±1**	**1±0**
AO-extractable polymers	**5±1**	**11±1**	**3±0**	**6±0**	13±10	41±16	**20±5**	**8±2**	**46±9**	**11±8**	**12±2**	**21±5**	1±1	2±0
KOH-extractable polymers	**2±0**	**5±0**	**1±0**	**2±0**	**2±0**	**14±2**	**4±0**	**6±1**	**83±1**	**60±4**	**8±1**	**12±1**	**0±0**	**1±0**
KOH-unextractable material[a], including	3±1	3±0	2±1	2±0	**6±1**	**10±0**	**50±3**	**60±2**	**32±1**	**21±1**	**5±0**	**4±0**	0±0	0±0
Cellulose-retained polymers [b]	3±1	3±0	2±0	2±1	**17±2**	**35±3**	w/o	w/o	**74±2**	**56±2**	3±1	2±1	1±0	1±0
Lignin-bound polymers [c]	8±1	10±1	**5±0**	**7±0**	**16±2**	**22±0**	**41±7**	**25±1**	18±6	22±2	12±1	13±1	1±0	1±0
mg/g DW														
Buffer-extractable polymers	**0.1±0.1**	**0.9±0.1**	**0.1±0.0**	**0.3±0.2**	**0.4±0.1**	**3.8±0.4**	0.1±0.1	0.2±0.1	**0.3±0.1**	**0.1±0.0**	**0.2±0.1**	**2.2±0.3**	**0.0±0.0**	**0.1±0.01**
AO-extractable polymers	0.2±0.0	0.2±0.0	0.1±0.0	0.1±0.0	0.4±0.3	0.8±0.2	**0.7±0.2**	**0.2±0.1**	**1.4±0.4**	**0.2±0.2**	0.4±0.1	0.4±0.2	tr	tr
KOH-extractable polymers	4.5±0.2	5.7±0.9	**1.1±0.1**	**2.7±0.4**	**3.5±0.6**	**18.6±3.7**	**9.9±0.8**	**8.5±0.2**	**170.3±19.9**	**72.2±9.3**	18.1±3.0	16.5±2.1	**0.7±0.2**	**1.8±0.3**
KOH-unextractable material[a], including	1.3±0.4	1.6±0.4	0.8±0.3	0.9±0.4	**2.6±0.4**	**5.8±1.4**	**20.1±3.4**	**34.2±5.7**	11.9±1.9	11.3±2.7	2.4±0.5	2.4±0.7	0.1±0.0	0.2±0.1
Cellulose-retained polymers[b]	0.2±0.0	0.3±0.0	0.1±0.0	0.1±0.0	**1.4±0.3**	**2.8±0.4**	w/o	w/o	**5.4±0.8**	**4.1±0.1**	0.3±0.1	0.2±0.1	0.1±0.0	0.1±0.0
Lignin-bound polymers[c]	**0.7±0.1**	**0.3±0.0**	**0.4±0.1**	**0.2±0.0**	**1.4±0.1**	**0.8±0.0**	**3.8±1.2**	**0.9±0.0**	1.6±0.6	0.8±0.1	**1.2±0.1**	**0.5±0.1**	**0.1±0.0**	**tr**

w/o – without Glc, since Glc could have been derived from cellulose during the procedure used; tr- trace.

[a] obtained by TFA hydrolysis of the pellet remaining after AO and KOH treatments;

[b] obtained by TFA hydrolysis of polymers collected after dissolution of KOH-unextractable pellets with LiCl in DMA and cellulose degradation;

[c] obtained by TFA hydrolysis of pellets remaining after dissolution of KOH-unextractable pellets with LiCl in DMA and cellulose degradation.

Values with significant differences between NW and TW samples according to Student's test are marked in bold.

Supplemental Material

Figure S1. Scheme of the sequential extraction of cell walls, designation of analyzed fractions and indication of performed analyses.

Figure S2. Immunolocalization of cell wall polysaccharides in fibers of normal wood (to the left) and tension wood (to the right) with RU2 antibody **(A, B)**, LM15 antibody **(C, D)**, and LM21 antibody **(E, F)**. CML – compound middle lamella, CW – cell wall, GL – G-layer, S1 and S2 – secondary cell wall layers. Silver enhancement was applied for different times (2-5 min) leading to different sizes of particles. Scale bar: 1.0 μm.

Parsed Citations

Åkerholm M,Salmén L (2001) Interactions between wood polymers studied by dynamic FT-IR spectroscopy. Polymer 42: 963-969
Pubmed: Author and Title
CrossRef: Author and Title
Google Scholar: Author Only Title Only Author and Title

Andème-Onzighi C,Girault R,His I,Morvan C,Driouich A (2000) Immunocytochemical characterization of early-developing flax fibre cell walls. Protoplasma 213: 235-245
Pubmed: Author and Title
CrossRef: Author and Title
Google Scholar: Author Only Title Only Author and Title

Andersson-Gunnerås S,Mellerowicz EJ,Love J,Segerman B,Ohmiya Y,Coutinho PM, Nilsson P,Henrissat B,Moritz T,Sundberg B (2006) Biosynthesis of cellulose enriched tension wood in Populus: global analysis of transcripts and metabolites identifies biochemical and developmental regulators in secondary wall biosynthesis. Plant J 45: 144-165
Pubmed: Author and Title
CrossRef: Author and Title
Google Scholar: Author Only Title Only Author and Title

Arend M (2008) Immunolocalization of (1,4)-beta-galactan in tension wood fibers of poplar. Tree Physiol 28: 1263-1267
Pubmed: Author and Title
CrossRef: Author and Title
Google Scholar: Author Only Title Only Author and Title

Baba K,Park YW,Kaku T, et al (2009) Xyloglucan for generating tensile stress to bend tree stem. Molecular Plant 2: 893-903
Pubmed: Author and Title
CrossRef: Author and Title
Google Scholar: Author Only Title Only Author and Title

Banasiak A,Ibatullin FM,Brumer H,Mellerowicz EJ (2014) Glycoside hydrolase activities in cell walls of sclerenchyma cells in the inflorescence stems of Arabidopsis thaliana visualized in situ. Plants 3: 513-525
Pubmed: Author and Title
CrossRef: Author and Title
Google Scholar: Author Only Title Only Author and Title

Barton CJ,Tailford LE,Welchman H,Zhang Z,Gilbert HJ,Dupree P,Goubet F (2006) Enzymatic fingerprinting of Arabidopsis pectic polysaccharides using PACE- polysaccharide analysis by carbohydrate gel electrophoresis. Planta 224:163-74
Pubmed: Author and Title
CrossRef: Author and Title
Google Scholar: Author Only Title Only Author and Title

Bourquin V,Nishikubo N,Abe H,Brumer H,Denman S,Eklund M,Christiernin M,Teeri TT,Sundberg B,Mellerowicz EJ (2002) Xyloglucan endotransglycosylases have a function during the formation of secondary cell walls of vascular tissues. Plant Cell 14: 3073-3088
Pubmed: Author and Title
CrossRef: Author and Title
Google Scholar: Author Only Title Only Author and Title

Bowling AJ,Vaughn KC (2008) Immunocytochemical characterization of tension wood: gelatinous fibers contain more than just cellulose. Am J Bot 95: 655-663
Pubmed: Author and Title
CrossRef: Author and Title
Google Scholar: Author Only Title Only Author and Title

Bowling AJ,Vaughn KC (2009) Gelatinous ?bers are widespread in tendrils and vines. Am J Bot 96: 719-727
Pubmed: Author and Title
CrossRef: Author and Title
Google Scholar: Author Only Title Only Author and Title

Bozzola JJ,Russell LD (1999) Electron microscopy: Principles and techniques for biologists, 2nd edn. Jones and Barlett, Boston, MA
Pubmed: Author and Title
CrossRef: Author and Title
Google Scholar: Author Only Title Only Author and Title

Burgert I,Fratzl P (2009) Plants control the properties and actuation of their organs through the orientation of cellulose fibrils in their cell walls. Integr Comp Biol 49: 69-79
Pubmed: Author and Title
CrossRef: Author and Title
Google Scholar: Author Only Title Only Author and Title

Chang SS,Clair B,Ruelle J,Beauchene J,Di Renzo F,Quignard F,Zhao GJ,Yamamoto H,Gril J (2009) Mesoporosity as a new parameter for understanding tension stress generation in trees. J Exp Bot 60: 3023-3030
Pubmed: Author and Title
CrossRef: Author and Title
Google Scholar: Author Only Title Only Author and Title

Chang SS,Quignard F,Alméras T,Clair B (2015) Mesoporosity changes from cambium to mature tension wood: a new step toward the understanding of maturation stress generation in trees. New Phytol 205:1277-1287.

Pubmed: Author and Title
CrossRef: Author and Title
Google Scholar: Author Only Title Only Author and Title

Clair B,Thibaut B (2001) Shrinkage of the gelatinous layer of poplar and beech tension wood. IAWA J 22: 121-131
Pubmed: Author and Title
CrossRef: Author and Title
Google Scholar: Author Only Title Only Author and Title

Clair B,Thibaut B,Sugiyama J (2005) On the detachment of the gelatinous layer in tension wood fiber. J Wood Sci 51: 218-221
Pubmed: Author and Title
CrossRef: Author and Title
Google Scholar: Author Only Title Only Author and Title

Clair B,Alméras T,Yamamoto H,Okuyama T,Sugiyama J (2006) Mechanical behavior of cellulose microfibrils in tension wood, in relation with maturation stress generation. Biophys J 91: 1128-1135
Pubmed: Author and Title
CrossRef: Author and Title
Google Scholar: Author Only Title Only Author and Title

Clair B,Gril J,Di Renzo F,Yamamoto H,Quignard F (2008) Characterization of a gel in the cell wall to elucidate the paradoxical shrinkage of tension wood. Biomacromolecules 9: 494-498
Pubmed: Author and Title
CrossRef: Author and Title
Google Scholar: Author Only Title Only Author and Title

Clair B,Almeras T,Pilate G,Jullien D,Sugiyama J,Riekel C (2011) Maturation stress generation in poplar tension wood studied by synchrotron radiation microdiffraction. Plant Physiol 155: 562-570
Pubmed: Author and Title
CrossRef: Author and Title
Google Scholar: Author Only Title Only Author and Title

Cronier D,Monties B,Chabbert B (2005) Structure and chemical composition of bast fibers isolated from developing hemp stem. J Agric Food Chem 53: 8279-8289
Pubmed: Author and Title
CrossRef: Author and Title
Google Scholar: Author Only Title Only Author and Title

Decou R,Lhernould S,Laurans F,Sulpice E,Leplé J-C,Déjardin A,Pilate G,Costa G (2009) Cloning and expression analysis of a wood-associated xylosidase gene (PtaBXL1) in poplar tension wood. Phytochem 70: 163-172
Pubmed: Author and Title
CrossRef: Author and Title
Google Scholar: Author Only Title Only Author and Title

Dubois M,Gilles KA,Hamilton JK (1956) Colorimetric method for determination of sugars and related substances. Analyt Chem 28: 350-356
Pubmed: Author and Title
CrossRef: Author and Title
Google Scholar: Author Only Title Only Author and Title

Fagerstedt KV,Mellerowicz E,Gorshkova T,Ruel K,Joseleau J-P (2014) Cell Wall Polymers in Reaction Wood. In B Gardiner, J Barnett, P Saranpää, J Gril, eds, Biology of Reaction Wood, Springer Series in Wood Science, Springer-Verlag Berlin Heidelberg, pp 37-106
Pubmed: Author and Title
CrossRef: Author and Title
Google Scholar: Author Only Title Only Author and Title

Fang CH,Clair B,Gril J,Liu SQ (2008) Growth stresses are highly controlled by the amount of G-layer in poplar tension wood. IAWA J 29: 237-246
Pubmed: Author and Title
CrossRef: Author and Title
Google Scholar: Author Only Title Only Author and Title

Fournier M,Alméras T,Clair B,Gril J (2014) Biomechanical action and biological functions. In B Gardiner, J Barnett, P Saranpää, J Gril, eds, Biology of Reaction Wood, Springer Series in Wood Science, Springer-Verlag Berlin Heidelberg, pp 139-169
Pubmed: Author and Title
CrossRef: Author and Title
Google Scholar: Author Only Title Only Author and Title

Furuya N,Takahashi S,Miyazaki M (1970) The chemical composition of the gelatinous layer from the tension wood of Populus euroamericana. Mokuzai Gakkaishi 16: 26-30
Pubmed: Author and Title
CrossRef: Author and Title
Google Scholar: Author Only Title Only Author and Title

Gierlinger N,Schwanninger M (2006) Chemical imaging of poplar wood cell walls by confocal Raman microscopy. Plant Physiol 140: 1246-1254
Pubmed: Author and Title
CrossRef: Author and Title
Google Scholar: Author Only Title Only Author and Title

Gorshkova T,Morvan C (2006) Secondary cell-wall assembly in flax phloem fibers: role of galactans. Planta 223: 149-158
Pubmed: Author and Title
CrossRef: Author and Title
Google Scholar: Author Only Title Only Author and Title

Gorshkova TA,Wyatt SE,Salnikov VV,Gibeaut DM,Ibragimov MR,Lozovaya VV,Carpita NC (1996) Cell-wall polysaccharides of developing flax plants. Plant Physiol 110: 721-729
Pubmed: Author and Title
CrossRef: Author and Title
Google Scholar: Author Only Title Only Author and Title

Gorshkova TA,Salnikov VV,Pogodina NM,Chemikosova SB,Yablokova EV,Ulanov AV,Ageeva MV,van Dam JEG,Lozovaya VV (2000) Composition and distribution of cell wall phenolic compounds in the ?ax (Linum usitatissimum L.) stem tissues. Ann Bot 85: 477-486
Pubmed: Author and Title
CrossRef: Author and Title
Google Scholar: Author Only Title Only Author and Title

Gorshkova TA,Chemikosova SB,Salnikov VV,Pavlencheva NV,Gurjanov OP,Stolle-Smits T,van Dam JEG (2004) Occurrence of cell-specific galactan is coinciding with bast fibre developmental transition in flax. Ind Crop Prod 19: 217-224
Pubmed: Author and Title
CrossRef: Author and Title
Google Scholar: Author Only Title Only Author and Title

Gorshkova TA,Gurjanov OP,Mikshina PV,Ibragimova NN,Mokshina NE,Salnikov VV,Ageeva MV,Amenitskii SI,Chernova TE,Chemikosova SB (2010) Specific type of secondary cell wall formed by plant fibers. Rus J Plant Physiol 57: 328-341
Pubmed: Author and Title
CrossRef: Author and Title
Google Scholar: Author Only Title Only Author and Title

Gorshkova T,Brutch N,Chabbert B,Deyholos M,Hayashi T,Lev-Yadun S,Mellerowicz EJ,Morvan C,Neutelingsi G,Pilate G (2012) Plant fiber formation: state of the art, recent and expected progress, and open questions. Cr Rev Plant Sci 31 (3): 201-228
Pubmed: Author and Title
CrossRef: Author and Title
Google Scholar: Author Only Title Only Author and Title

Goswami L,Dunlop JWC,Jungnikl K,Eder M,Gierlinger N,Coutand C,Jeronimidis G,Fratzl P,Burgert I (2008) Stress generation in tension wood of poplar is based on the lateral swelling power of the G-layer. Plant J 56: 531-538
Pubmed: Author and Title
CrossRef: Author and Title
Google Scholar: Author Only Title Only Author and Title

Goubet F,Jackson P,Deery MJ,Dupree P (2002) Polysaccharide analysis using carbohydrate gel electrophoresis: a method to study plant cell wall polysaccharides and polysaccharide hydrolases. Anal Biochem 300: 53-68
Pubmed: Author and Title
CrossRef: Author and Title
Google Scholar: Author Only Title Only Author and Title

Goubet F,Barton CJ,Mortimer JC,Yu X,Zhang Z,Miles GP,Richens J,Liepman AH,Seffen K,Dupree P (2009) Cell wall glucomannan in Arabidopsis is synthesised by CSLA glycosyltransferases, and in?uences the progression of embryogenesis. Plant J 60: 527-538
Pubmed: Author and Title
CrossRef: Author and Title
Google Scholar: Author Only Title Only Author and Title

Gurjanov OP,Gorshkova TA,Kabel M,Schols HA,van Dam JEG (2007) MALDI-TOF MS evidence for the linking of flax bast fibre galactan to rhamnogalacturonan backbone. Carbohydr Polym 67: 86-96
Pubmed: Author and Title
CrossRef: Author and Title
Google Scholar: Author Only Title Only Author and Title

Gurjanov OP,Ibragimova NN,Gnezdilov OI,Gorshkova TA (2008) Polysaccharides, tightly bound to cellulose in the cell wall of flax bast fibre: Isolation and identification. Carbohydr Res 72: 719-729
Pubmed: Author and Title
CrossRef: Author and Title
Google Scholar: Author Only Title Only Author and Title

Hainfeld JF,Powell RD (2000) New frontiers in gold labeling. J Histochem Cytochem 48: 471-480
Pubmed: Author and Title
CrossRef: Author and Title
Google Scholar: Author Only Title Only Author and Title

Hayashi T,Kaida R,Kaku T,Baba K (2010) Loosening xyloglucan prevents tensile stress in tree stem bending but accelerates the enzymatic degradation of cellulose. Rus J Plant Physiol 57: 316-320
Pubmed: Author and Title
CrossRef: Author and Title
Google Scholar: Author Only Title Only Author and Title

Hedenström M,Wiklund-Lindström S,Oman T,Lu F,Gerber L,Schatz P,Sundberg B,Ralph J (2009) Identification of lignin and polysaccharide modifications in Populus wood by chemometric analysis of 2D NMR spectra from dissolved cell walls. Mol Plant 2: 933-942
Pubmed: Author and Title

CrossRef: Author and Title
Google Scholar: Author Only Title Only Author and Title

Ibatullin FM,Banasiak A,Baumann MJ,Gre?e L,Takahashi J,Mellerowicz EJ,Brumer H (2009) A real-time ?uorogenic assay for the visualization of glycoside hydrolase activity in planta. Plant Physiol 151: 1741-1750
Pubmed: Author and Title
CrossRef: Author and Title
Google Scholar: Author Only Title Only Author and Title

Jensen MH,Otten H,Christensen U,Borchert TV,Christensen LLH,Larsen S,Leggio LL (2010) Structural and biochemical studies elucidate the mechanism of rhamnogalacturonan lyase from Aspergillus aculeatus. J Mol Biol 404: 100-111
Pubmed: Author and Title
CrossRef: Author and Title
Google Scholar: Author Only Title Only Author and Title

Jones L,Seymour GB,Knox JP (1997) Localization of pectic galactan in tomato cell walls using a monoclonal antibody specific to (1?4)-beta-D-galactan. Plant Physiol 113: 1405-1412
Pubmed: Author and Title
CrossRef: Author and Title
Google Scholar: Author Only Title Only Author and Title

Joseleau J-P,Imai T,Kuroda K,Ruel K (2004) Detection in situ and characterization of lignin in the G-layer of tension wood fibres of Populus deltoides. Planta 219: 338-345
Pubmed: Author and Title
CrossRef: Author and Title
Google Scholar: Author Only Title Only Author and Title

Kaku T,Serada S,Baba K,Tanaka F,Hayashi T (2009) Proteomic analysis of the G-Layer in poplar tension wood. J Wood Sci 55: 250-257
Pubmed: Author and Title
CrossRef: Author and Title
Google Scholar: Author Only Title Only Author and Title

Kim JS,Daniel G (2012) Distribution of glucomannans and xylans in poplar xylem and their changes under tension stress. Planta 236: 35-50.
Pubmed: Author and Title
CrossRef: Author and Title
Google Scholar: Author Only Title Only Author and Title

Knox JP,Linstead PJ,Peart J,Cooper C,Roberts K (1991) Developmentally-regulated epitopes of cell surface arabinogalactan-proteins and their relation to root tissue pattern formation. Plant J 1: 317-326
Pubmed: Author and Title
CrossRef: Author and Title
Google Scholar: Author Only Title Only Author and Title

Kudla J,Batistic O,Hashimoto K (2010) Calcium signals: The lead currency of plant information processing. Plant Cell 22: 541-563
Pubmed: Author and Title
CrossRef: Author and Title
Google Scholar: Author Only Title Only Author and Title

Kuo CM,Timell TE. 1969. Isolation and characterization of a galactan from tension wood of American Beech (Fagus grandifolia Ehrl.). Svensk Papperstidn 72: 703-716.
Pubmed: Author and Title
CrossRef: Author and Title
Google Scholar: Author Only Title Only Author and Title

Lafarguette F,Leplé J-Ch,Déjardin A,Laurans F,Costa G,Lesage-Descauses M-C,Pilate G (2004) Poplar genes encoding fasciclin-like arabinogalactan proteins are highly expressed in tension wood. New Phytol 164: 107-121
Pubmed: Author and Title
CrossRef: Author and Title
Google Scholar: Author Only Title Only Author and Title

Lamport DT,Varnai P (2013) Periplasmic arabinogalactan glycoproteins act as a calcium capacitor that regulates plant growth and development. New Phytol 197: 58-64
Pubmed: Author and Title
CrossRef: Author and Title
Google Scholar: Author Only Title Only Author and Title

Love GD,Snape CE,Jarvis MC,Morrison IM (1994) Determination of phenolic structures in flax fibre by solid state 13C NMR. Phytochem 35: 489-492
Pubmed: Author and Title
CrossRef: Author and Title
Google Scholar: Author Only Title Only Author and Title

Marcus SE,Verhertbruggen Y,Herve C,Ordaz-Ortiz JJ,Farkas V,Pedersen HL,Willats WGT,Knox JP (2008) Pectic homogalacturonan masks abundant sets of xyloglucan epitopes in plant cell walls. BMC Plant Biol 8: 60-71
Pubmed: Author and Title
CrossRef: Author and Title
Google Scholar: Author Only Title Only Author and Title

Marcus SE,Blake AW,Benians TAS et al. (2010) Restricted access of proteins to mannan polysaccharides in intact plant cell walls.

Plant J 64: 191-203
Pubmed: Author and Title
CrossRef: Author and Title
Google Scholar: Author Only Title Only Author and Title

McCartney L,Marcus SE,Knox JP (2005) Monoclonal antibodies to plant cell wall xylans and arabinoxylans. J Histochem and Cytochem 53: 543-546
Pubmed: Author and Title
CrossRef: Author and Title
Google Scholar: Author Only Title Only Author and Title

Meier H (1962). Studies on galactan from tension wood of beech (Fagus silvatica L.). Acta Chem Scand 16: 2275-2283
Pubmed: Author and Title
CrossRef: Author and Title
Google Scholar: Author Only Title Only Author and Title

Mellerowicz EJ,Baucher M,Sundberg B,Boerjan W (2001) Unraveling cell wall formation in the woody dicot stem. Plant Mol Biol 47: 239-274
Pubmed: Author and Title
CrossRef: Author and Title
Google Scholar: Author Only Title Only Author and Title

Mellerowicz EJ,Immerzeel P,Hayashi T (2008) Xyloglucan - the molecular muscle of trees. An Bot 101: 659-665
Pubmed: Author and Title
CrossRef: Author and Title
Google Scholar: Author Only Title Only Author and Title

Mellerowicz EJ,Gorshkova TA (2012) Tensional stress generation in gelatinous fibres: a review and possible mechanism based on cell-wall structure and composition. J Exp Bot 63: 551-565
Pubmed: Author and Title
CrossRef: Author and Title
Google Scholar: Author Only Title Only Author and Title

Mikshina PV,Chemikosova SB,Mokshina NE,Ibragimova NN,Gorshkova TA (2009) Free galactose and galactosidase activity in the course of flax fiber development. Rus J Plant Physiol 56: 58-67
Pubmed: Author and Title
CrossRef: Author and Title
Google Scholar: Author Only Title Only Author and Title

Mikshina PV,Gurjanov OP,Mukhitova FK,Petrova AA,Shashkov AS,Gorshkova TA (2012) Structural details of pectic galactan from the secondary cell walls of flax (Linum usitatissimum L.) phloem fibres. Carbohydr Polym 87: 853-861
Pubmed: Author and Title
CrossRef: Author and Title
Google Scholar: Author Only Title Only Author and Title

Mikshina PV,Idiyatullin BZ,Petrova AA,Shashkov AS,Zuev YuF,Gorshkova TA (2015) Physicochemical properties of complex rhamnogalacturonan I from gelatinous cell walls of flax fibers. Carbohydr Polym 117: 853-861
Pubmed: Author and Title
CrossRef: Author and Title
Google Scholar: Author Only Title Only Author and Title

Mizrachi E,Maloney VJ,Silberbauer J,Hefer CA,Berger DK, Mans?eld SD, Myburg AA (2014) Investigating the molecular underpinnings underlying morphology and changes in carbon partitioning during tension wood formation in Eucalyptus. New Phytol doi: 10.1111/nph.13152. PMID: 25388807
Pubmed: Author and Title
CrossRef: Author and Title
Google Scholar: Author Only Title Only Author and Title

Mokshina NE,Ibragimova NN,Salnikov VV,Amenitskii SI,Gorshkova TA (2012) Galactosidase of plant fibers with gelatinous cell wall: Identification and localization. Rus J Plant Physiol 59(2): 246-254
Pubmed: Author and Title
CrossRef: Author and Title
Google Scholar: Author Only Title Only Author and Title

Müller M,Burghammer M,Sugiyama J (2006) Direct investigation of the structural properties of tension wood cellulose microfibrils using microbeam X-ray fibre diffraction. Holzforschung 60: 474-479
Pubmed: Author and Title
CrossRef: Author and Title
Google Scholar: Author Only Title Only Author and Title

Nishikubo N,Awano T,Banasiak A, et al (2007) Xyloglucan endo-transglycosylase (XET) functions in gelatinous layers of tension wood fibers in poplar - A glimpse into the mechanism of the balancing act of trees. Plant Cell Physiol 48: 843-855
Pubmed: Author and Title
CrossRef: Author and Title
Google Scholar: Author Only Title Only Author and Title

Norberg PH,Meier H (1966) Physical and chemical properties of Gelatinous layer in tension wood fibres of Aspen (Populus tremula L.). Holzforsehung 20: 174-178
Pubmed: Author and Title
CrossRef: Author and Title
Google Scholar: Author Only Title Only Author and Title

Olsson A-M,Bjurhager I,Gerber L,Sundberg B,Salmén L (2011) Ultra-structural organisation of cell wall polymers in normal and tension wood of aspen revealed by polarisation FTIR microspectroscopy. Planta 233: 1277-1286
Pubmed: Author and Title
CrossRef: Author and Title
Google Scholar: Author Only Title Only Author and Title

Pattathil S,Avci U,Baldwin D,Swennes AG et al. (2010) A comprehensive toolkit of plant cell wall glycan-directed monoclonal antibodies. Plant Physiol 153: 514-525
Pubmed: Author and Title
CrossRef: Author and Title
Google Scholar: Author Only Title Only Author and Title

Paux E,Carocha V,Marques C,de Sousa AM,Borralho N,Sivadon P,Grima-Pettenati J (2005) Transcript profiling of Eucalyptus xylem genes during tension wood formation. New Phytol 167: 89-100
Pubmed: Author and Title
CrossRef: Author and Title
Google Scholar: Author Only Title Only Author and Title

Pilate G,Dejardin A,Laurans F,Leple J-C (2004) Tension wood as a model for functional genomics of wood formation. New Phytol 164: 63-72
Pubmed: Author and Title
CrossRef: Author and Title
Google Scholar: Author Only Title Only Author and Title

Ralet M-C,Tranquet O,Poulain D,Moise A,Guillon F (2010) Monoclonal antibodies to rhamnogalacturonan I backbone. Planta 231: 1373-1383
Pubmed: Author and Title
CrossRef: Author and Title
Google Scholar: Author Only Title Only Author and Title

Reynolds ES (1963) The use of lead citrate at high pH as an electron-opaque stain in electron microscopy. J Cell Biol 17: 208-213
Pubmed: Author and Title
CrossRef: Author and Title
Google Scholar: Author Only Title Only Author and Title

Roach MJ,Deyholos MK (2007) Microarray analysis of flax (Linum usitatissimum L.) stems identifies transcripts enriched in fibre-bearing phloem tissues. Mol Genet Genomics 278: 149-165
Pubmed: Author and Title
CrossRef: Author and Title
Google Scholar: Author Only Title Only Author and Title

Roach MJ,Mokshina NY,Badhan A,Snegireva AV,Hobson N,Deyholos MK,Gorshkova TA (2011) Development of cellulosic secondary walls in flax fibers requires beta-galactosidase. Plant Physiol 156: 1351-1363
Pubmed: Author and Title
CrossRef: Author and Title
Google Scholar: Author Only Title Only Author and Title

Ruel K,Barnoud F (1978) Research on the quantitative determination of tension wood in beech. Statistical significance of the galactose content. Holzforschung 32(5): 149-156
Pubmed: Author and Title
CrossRef: Author and Title
Google Scholar: Author Only Title Only Author and Title

Rüggeberg M,Saxe F,Metzger TH,Sundberg B,Fratzl P,Burgert I (2013) Enhanced cellulose orientation analysis in complex model plant tissues. J Struct Biol 183(3): 419-428
Pubmed: Author and Title
CrossRef: Author and Title
Google Scholar: Author Only Title Only Author and Title

Salmén L,Burgert I (2009) Cell wall features with regard to mechanical performance. A review. Holzforschung 63: 121-129
Pubmed: Author and Title
CrossRef: Author and Title
Google Scholar: Author Only Title Only Author and Title

Salnikov VV,Ageeva MV,Gorshkova TA (2008) Homofusion of Golgi vesicles in flax phloem fibers during formation of gelatinous secondary cell wall. Protoplasma 233 (3-4): 269-273
Pubmed: Author and Title
CrossRef: Author and Title
Google Scholar: Author Only Title Only Author and Title

Sandquist D,Filonova L,von Schantz L,Ohlin M,Daniel G (2010) Microdistribution of xyloglucan in differentiating poplar cells. BioResources 5: 796-807
Pubmed: Author and Title
CrossRef: Author and Title
Google Scholar: Author Only Title Only Author and Title

Schreiber N,Gierlinger N,Putz N,Fratzl P,Neinhuis C,Burgert I (2010) G-fibres in storage roots of Trifolium pretense (Fabaceae): tensile stress generators for contraction. Plant J 61: 854-861
Pubmed: Author and Title
CrossRef: Author and Title

Google Scholar: Author Only Title Only Author and Title

Takata R,Tokita K,Mori S, et al. (2010) Degradation of carbohydrate moieties of arabinogalactan-proteins by glycoside hydrolases from Neurospora crassa. Carbohydr Res 345: 2516-2522
Pubmed: Author and Title
CrossRef: Author and Title
Google Scholar: Author Only Title Only Author and Title

Tan L,Varnai P,Lamport DTA,Yuan C,Xu J,Qiu F,Kieliszewski MJ (2010) Plant O-hydroxyproline arabinogalactans are composed of repeating trigalactosyl subunits with short bifurcated side chains. J Biol Chem 285: 24575-24583
Pubmed: Author and Title
CrossRef: Author and Title
Google Scholar: Author Only Title Only Author and Title

Talmage KW,Keegstra K,Bauer WO,Albersheim P (1973) The structure of plant cell walls. I. The macromolecular components of the pectic polysaccharides II. Plant Physiol 51: 158-173
Pubmed: Author and Title
CrossRef: Author and Title
Google Scholar: Author Only Title Only Author and Title

Tryfona T,Liang HC,Kotake T,Tsumuraya Y,Stephens E,Dupree P (2012) Structural characterization of Arabidopsis leaf arabinogalactan polysaccharides. Plant Physiol 160: 563-666
Pubmed: Author and Title
CrossRef: Author and Title
Google Scholar: Author Only Title Only Author and Title

Tsumuraya Y,Mochizuki N,Hashimoto Y,Kovác P (1990) Purification of an exo-ß-(1?3)-D-galactanase of Irpex lacteus (Polyporus tulipiferae) and its action on arabinogalactan-proteins. J Biol Chem 265: 7207-7215
Pubmed: Author and Title
CrossRef: Author and Title
Google Scholar: Author Only Title Only Author and Title

Wardrop AB,Dadswell HE (1948) The nature of reaction wood. I. The structure and properties of tension wood fibres. Aust J Sci Res Ser B 1: 4-19
Pubmed: Author and Title
CrossRef: Author and Title
Google Scholar: Author Only Title Only Author and Title

Yamamoto H,Abe K,Arakawa Y,Okuyama T,Gril J (2005) Role of the gelatinous layer (G-layer) on the origin of the physical properties of the tension wood of Acer sieboldianum. J Wood Sci 51: 222-233
Pubmed: Author and Title
CrossRef: Author and Title
Google Scholar: Author Only Title Only Author and Title

Yamamoto H,Ruelle J,Arakawa Y,Yoshida M,Clair B,Gril J (2009) Origin of the characteristic hygro-mechanical properties of gelatinous layer in tension wood from Kunugi oak (Quercus acutissima). Wood Sci Technol 44: 149-163
Pubmed: Author and Title
CrossRef: Author and Title
Google Scholar: Author Only Title Only Author and Title